MORPHOMETRIC ANALYSIS OF BIOSTRATIGRAPHICALLY SIGNIFICANT FUSULINID FORAMINIFERAN GENUS TRITICITES ACROSS THE PENNSYLVANIAN-PERMIAN BOUNDARY IN THE CENTRAL AND SOUTHWESTERN UNITED STATES

A Thesis

by

EILEAH RENEE SIMS

Submitted to the Office of Graduate and Professional Studies of
Texas A&M University
in partial fulfillment of the requirements for the degree of

MASTER OF SCIENCE

Chair of Committee,	Christina L. Belanger
Committee Members,	Anne Raymond
	Anna Michelle Lawing
Head of Department,	Julie Newman

August 2020

Major Subject: Geology

ABSTRACT

Fusulinid foraminifera are commonly used for Late Paleozoic biostratigraphic correlations in the Central and Southwestern United States instead of conodonts due to the high abundance of fusulinids in Late Paleozoic carbonates. These correlations rely on consistent identification of biostratigraphically significant species using morphological characters. However, these characters are often translated into qualitative descriptors such as, “inflated”, “elongated” and “more fluted”, which can lead to discrepancies among taxonomists and cause biostratigraphic disagreements. Quantitative morphometric studies can help make taxonomy replicable among workers. Here, we use 14 linear measurements to define the morphology of 18 species within the biostratigraphically important genus *Triticites*. A canonical variates analysis (CVA) shows that while specimens of a given species occupy similar morphospace, congenerics overlap considerably in morphospace, and thus cross-validation showed that species prediction based on these measurements was poor (~27%). However, a linear discriminant analysis (LDA) of specimen measurements correctly predicted whether specimens were from the Virgilian (latest Pennsylvanian) or Newwellian-Nealian (earliest Permian) in ~77% of cases. This indicates that incorrect predictions most often occurred among specimens of similar age. The LDA further revealed morphological differences between specimens of different stratigraphic age, which are primarily driven by proloculus size relative to the overall size of the organism at the 4th volution. This may reflect a change within *Triticites* from an r-selected reproductive strategy in the

latest Pennsylvanian to a K-selected reproductive strategy in the earliest Permian in response to changing environmental conditions. This morphological change is replicated in all four tested North American basins and could indicate that the environmental changes across the Pennsylvanian-Permian boundary were at the continent-scale. This morphological shift is potentially useful for biostratigraphy because it does not depend on species identification and is recognizable in analyses blind to stratigraphic age association.

DEDICATION

For Mom and Dad, who taught me that hard work makes a difference and to never give up on your dreams.

ACKNOWLEDGEMENTS

I would like to thank Susan Butts and Jessica Utrup at the Yale Peabody Museum of Natural History and Science; Nicole Ridgwell and Spencer G. Lucas at the New Mexico Museum of Natural History and Science for allowing access to museum collections.

I also thank Spencer G. Lucas and Arthur Donovan for critical information regarding fusulinid biostratigraphy and Pennsylvanian-Permian stratigraphy in general. I would also like to thank David W. Bapst, Christina L. Belanger, Anna Michelle Lawing, Anne Raymond, Ethan L. Grossman, and Melanie J. Hopkins for their help in understanding the methods used for this research and understanding the implications for the results.

CONTRIBUTORS AND FUNDING SOURCES

Contributors

This work was supervised by a thesis committee consisting of Drs. Christina L Belanger and Anne Raymond of the Department of Geology and Geophysics and Dr. Anna Michelle Lawing of the Department of Ecosystem Science and Management.

All other work conducted for the thesis was completed by the student independently.

Funding

Graduate study was funded by a fellowship from Texas A&M University and the David Worthington Family Named Grant from the AAPG Foundation Grants-In-Aid Program.

This work was also made possible by a travel grant from the Yale Peabody Museum Division of Invertebrate Paleontology “Charles Schuchert and Carl O. Dunbar Grants-in-Aid Program for Invertebrate Paleontological Research.”

TABLE OF CONTENTS

Page

ABSTRACT ii

DEDICATION iv

ACKNOWLEDGEMENTS v

CONTRIBUTORS AND FUNDING SOURCES vi

TABLE OF CONTENTS vii

LIST OF FIGURES ix

LIST OF TABLES xi

1. INTRODUCTION 1

1.1. Study Area and Fusulinid Biostratigraphy 6

2. METHODS 9

2.1. Museum Specimens 9
2.2. Morphological Measurements 12
2.3. Quantitative Analyses 14
2.3.1. Multivariate Morphometrics for Species Delimitation 15
2.3.2. Temporal Comparisons of Morphology 16
2.3.3. Total Morphological Variation Within *Triticites* 16

3. RESULTS 18

3.1. Species-Based CVA 18
3.2. Temporally-Based LDA 24
3.3. Total Morphological Variation 27

4. DISCUSSION 31

4.1. Species Differentiation Among *Triticites* Species 31
4.2. Temporal Patterns in Morphology 33
4.3. Biostratigraphic Implications 39

5. CONCLUSIONS 41

REFERENCES 43

APPENDIX A CASE STUDY OF THE GRAY LIMESTONE MEMBER IN THE WOLFCAMP HILLS 55

APPENDIX B MORPHOLOGICAL DISTINCTIVENESS 57

B.1. Methods 57
B.2. Results 58
B.3. Discussion 59

LIST OF FIGURES

Page

Figure 1: Axial section of *Triticites gallowayi* (YPM IP 023672) depicting the long axis (half-length), short axis (radius vector), proloculus, tectum, and keriotheca (black scale bar = 1 mm). 2

Figure 2: Stratigraphic units seen in the Pedregosa (Big Hatchet Mountains), Southwest Orogrande, Delaware (Guadalupe Mountains and Glass Mountains), Midland and Midcontinent Basins. A) Showing current position of the GSSP Carboniferous-Permian Boundary based upon conodonts; coincides with base of the Nealian Substage of Ross, 1963. B) Position of Carboniferous-Permian Boundary implied by Wilde, 2006 on the basis of fusulinids; coincides with the base of the Newwellian Substage of Wilde, 2002. C) Stages and substages following Wilde, 2006 and Lucas et al., 2017b. Fusulinid foraminiferan biostratigraphic zones are shown for the South Delaware Basin adjacent to the corresponding stratigraphic units. Hatched areas indicate depositional hiatuses. 5

Figure 3: Late Pennsylvanian (300 Ma) paleogeographic map of North America (used with permission © 2013 Colorado Plateau Geosystems Inc.). Symbols indicate location of depositional basins used in this study. 7

Figure 4: Idealized schematic drawings of Fusulinid foraminiferan volutions with character definitions as seen on an axial section. A) Overall schematic of axial section of fusulinid test; B) Close-up of character definitions on fusulinid test. PR = inner proloculus radius; CH = chamber height along radius vector; HLE = half-length expansion; WT = wall thickness. C) Wall thickness includes the thickness of the tectum and the keriotheca. 14

Figure 5: Specimen scores from CVA Axes 1 and 2 (A, C, and E) and CVA Axes 1 and 3 (B, D, and F) showing specimen distribution in the morphospace. A-B) symbols correspond to species (legend below plots); C-D) symbols correspond to time bin; E-F) symbols correspond to basin (legend below plots). Gradational arrows on A and B indicate the direction in which the noted character measurements are increasing on each axis. Gradational arrows on A are the same on C and E. Gradational arrows on B are the same on D and F. 20

Figure 6: A) CVA Axis 1 scores for Virgilian and Newwellian-Nealian. B) LDA scores for Virgilian and Newwellian-Nealian. C) PCA Axis 2 scores for Virgilian and Newwellian-Nealian. Shaded box represents the

interquartile range (IQR). Lower box bound represents the 25th percentile (Q1) and the upper box bound represents the 75th percentile (Q3). Lower whisker represents the minimum values outside the IQR (Q1-1.5*IQR). Upper whisker represents the maximum values outside the IQR (Q3+1.5*IQR). Circles outside whiskers are the outliers. Thick middle line represents the median score. Notch represents 95% confidence around the median. 23

Figure 7: Stratigraphic age-based LDA scores of each studied basin (Pedregosa, Orogrande, Delaware, and Midcontinent) for the Virgilian and Newwellian-Nealian (n = number of specimens). Shaded box represents the interquartile range (IQR). Lower box bound represents the 25th percentile (Q1) and the upper box bound represents the 75th percentile (Q3). Lower whisker represents the minimum values outside the IQR (Q1-1.5*IQR). Upper whisker represents the maximum values outside the IQR (Q3+1.5*IQR). Circles outside whiskers are the outliers. Thick middle line represents the median score. 26

Figure 8: Specimen scores from PCA Axes 1 and 2 showing specimen distribution in the morphospace. A) symbols correspond to species (legend below plot); B) symbols correspond to time bin; C) symbols correspond to basin. Gradational arrows on A indicate the direction in which the noted character measurements are increasing on PCA Axis 2 and are the same for B and C 28

LIST OF TABLES

Page

Table 1: Table of the selected 18 biostratigraphically significant species of *Triticites* in the YPM and NMNMHS collections. For columns with the museum abbreviation, this is the number of specimens for a particular species in the museum's collections that were used in this study. The "Stratigraphic Unit" column shows the stratigraphic unit where each species was found, for the specimens used in this study. The "TOTAL" column shows the total number of specimens for each species used in this study. 10

Table 2: Character scalings for the first 3 axes of the species-based CVA and Stratigraphic age-based LDA and character loadings for the first 2 axes of the PCA. Bold scalings/loadings are the most positive and the most negative along each axis. PR = inner proloculus radius; CH = chamber height along radius vector; HLE = half-length expansion; WT = wall thickness. Numbers on character abbreviations correspond to the volution or growth stage number. 21

Table 3: Sample size, median, interquartile range (IQR), and Mann-Whitney U test results for stratigraphic age-based LDA scores in each time bin for each basin. 26

Table 4: Sample size, median, interquartile range (IQR), and Mann-Whitney U test results for PCA Axis 2 scores in each time bin for each basin. 30

1. INTRODUCTION

Biostratigraphy is essential to stratigraphic correlation across geographic regions as well as to observing the evolution of all life on Earth. Such correlations are dependent on consistent identification of species based upon their morphological characters (Dunbar and Skinner, 1937; Dunbar and Condra, 1927; Ross, 1963; Koepnick and Kaesler, 1974; Wilde, 2006; Groves and Reisdorph, 2009). Without quantitative support for morphological differences, the accuracy of identifications is often questioned (Arefifard, 2018) and differences in taxonomic identifications based on qualitative characteristics have led to biostratigraphic disagreements among workers and, therefore, the stratigraphic ages of certain rock units (Ross, 1994, 1995; Wilde, 2006; Koch and Frank, 2011; Lucas et al., 2017b; Zhang and Wang, 2018).

Fusulinid foraminifera are commonly used for biostratigraphic correlations among Carboniferous to Permian strata in North America due to their high abundance in shallow-water carbonates and increasing diversity during the late Paleozoic (Koch and Frank, 2011; BouDagher-Fadel, 2018). Most fusulinids have a fusiform, or seed-like, shape and add chambers to the sub-spherical embryonic (first) chamber, called the "proloculus", by coiling around the long axis (**Figure 1**) (Dunbar and Condra, 1927; BouDagher-Fadel, 2018). The superfamily Schwagerinoidea, which ranges from the middle Pennsylvanian to the middle Permian (BouDagher-Fadel, 2018), is important for recognizing the Pennsylvanian-Permian boundary (PPB) in shallow-marine strata. This superfamily contains only one family, Schwagerinidae, which includes genera with high

species turnover across the Pennsylvanian-Permian boundary (PPB) (BouDagher-Fadel, 2018). Schwagerinid fusulinids have large, fusiform to irregularly cylindrical tests with planispiral involute coiling (BouDagher-Fadel, 2018) and are common in shallow to intermediate carbonate platform facies (Ross, 1965, 1972; Groves et al., 2012; BouDagher-Fadel, 2018).

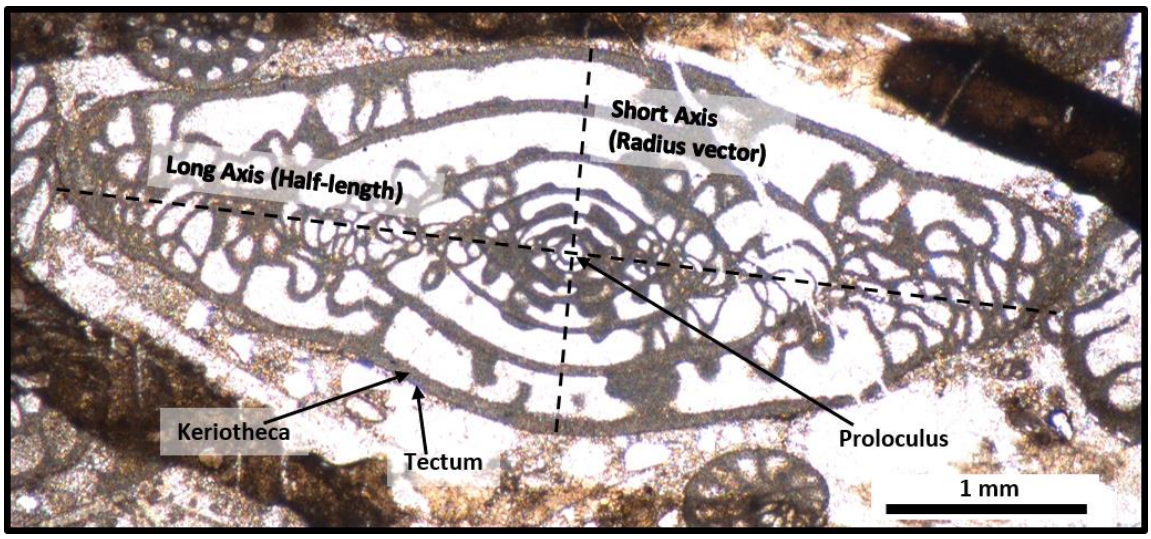

Figure 1: Axial section of *Triticites gallowayi* (YPM IP 023672) depicting the long axis (half-length), short axis (radius vector), proloculus, tectum, and keriotheca (black scale bar = 1 mm).

Although this group is biostratigraphically useful, the morphological characters used to distinguish species are largely qualitative, which can hinder consistent identification. For example, a considerable amount of debate about the identification of Permian versus Pennsylvanian species within the fusulinid genus *Triticites* has resulted

in age ambiguity in the uppermost late Pennsylvanian and lowermost early Permian strata (Ross, 1994; Wilde, 2006; Lucas et al., 2017b) (**Figure 2**). The lithostratigraphic units within the Wolfcampian stage (earliest Permian) in the Central and Southwestern United States have the highest estimated undiscovered unconventional oil reserve in the United States (Gaswirth, 2017), and, thus, precise correlation of these units has economic value.

Late Pennsylvanian and early Permian strata are divided into several fusulinid foraminiferan biostratigraphic zones (Ross, 1995; Wilde, 2006; Koch and Frank, 2011; Lucas et al., 2017b; Zhang and Wang, 2018). Identification of these zones of species above and below the PPB relies upon the ability to tell congeneric species apart. Typical characters used for the differentiation of species within *Triticites* are proloculus diameter, radius vector, half length, and wall thickness of each volution (growth stage) (Ross, 1963; Dunbar and Skinner, 1937; Dunbar and Condra, 1927; Koepnick and Kaesler, 1974; Wilde, 2006) (**Figure 1**). However, these objective characters are often translated into subjective qualitative descriptors such as, “inflated”, “elongated”, and “more fluted”, leading to disparate identifications among workers (Ross, 1963; Wilde, 2006; Lucas et al., 2017b). In addition to the biostratigraphic utility of *Triticites*, information about the morphology and stratigraphic ranges of these taxa are important to understand the evolution of later Permian fusulinids, given that *Triticites* is the hypothetical ancestor of this later Permian diversity (BouDagher-Fadel, 2018).

Here we use quantitative morphometric analyses to test the hypothesis that morphological characters can be used to consistently differentiate among *Triticites*

species across the PPB. We further test the hypothesis that significant morphological changes occur in *Triticites* across the PPB in the Central and Southwestern United States, and are, thus, distinct enough for use in biostratigraphic correlation. However, morphological variation among individuals could also reflect phenotypic plasticity, in response to environmental conditions, rather than evolution over time (Patzkowsky and Holland, 2012). If fusulinids respond to regional environmental changes, observed morphological changes may complicate biostratigraphy. Further, if fusulinids respond to local environmental changes, this could lead to diachronous morphological changes observed across basins, and, thus, lead to unreliable correlations. However, if fusulinid morphology responds to basin-wide or global environmental changes across the PPB, the morphological changes could be correlated. Therefore, we further test the hypotheses that morphological changes within *Triticites* are geographically consistent among multiple basins across the PPB and thus indicative of evolutionary processes or widespread environmental and ecological changes.

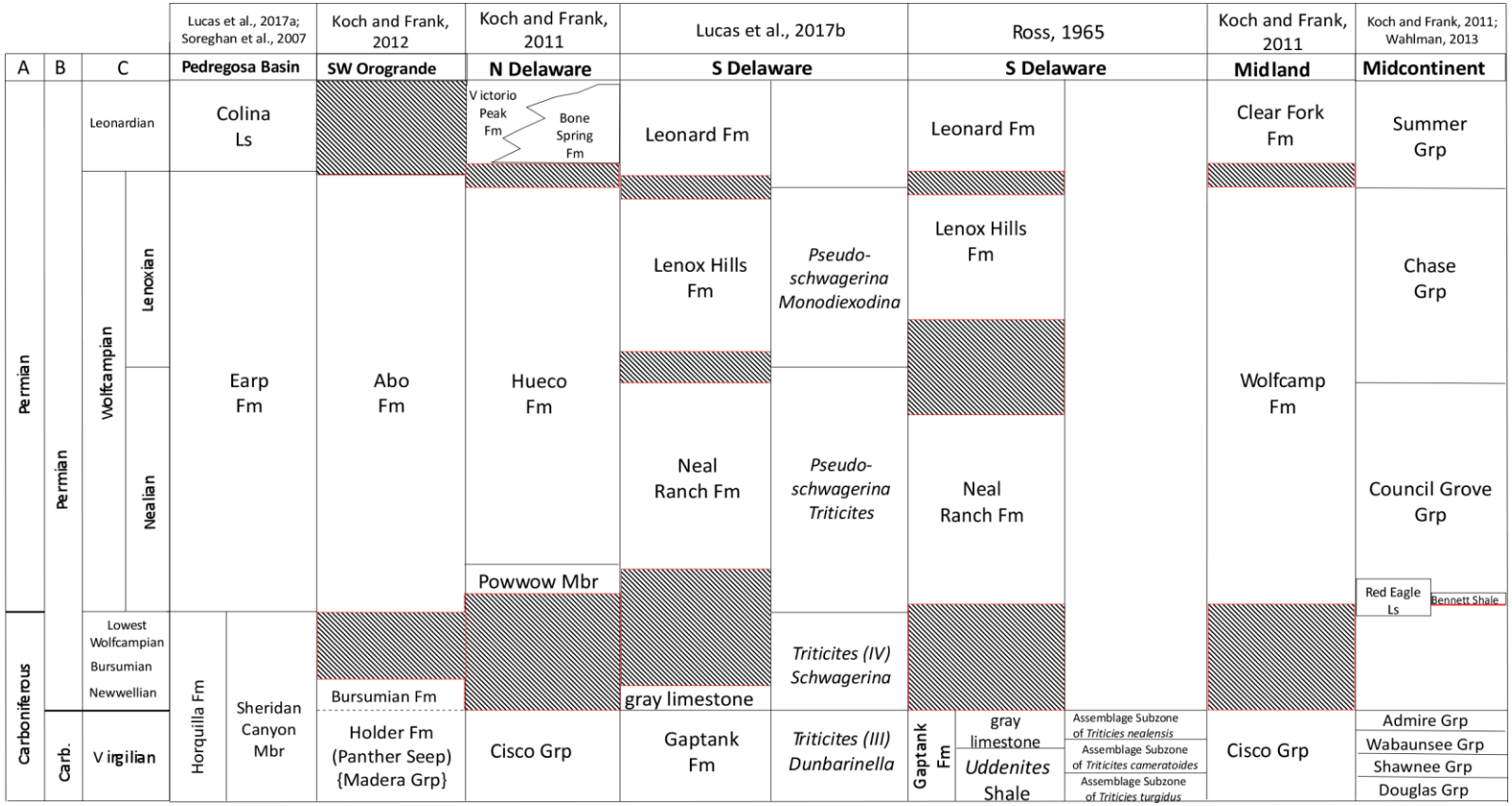

Figure 2: Stratigraphic units seen in the Pedregosa (Big Hatchet Mountains), Southwest Orogrande, Delaware (Guadalupe Mountains and Glass Mountains), Midland and Midcontinent Basins. A) Showing current position of the GSSP Carboniferous-Permian Boundary based upon conodonts; coincides with base of the Nealian Substage of Ross, 1963. B) Position of Carboniferous-Permian Boundary implied by Wilde, 2006 on the basis of fusulinids; coincides with the base of the Newwellian Substage of Wilde, 2002. C) Stages and substages following Wilde, 2006 and Lucas et al., 2017b. Fusulinid foraminiferan biostratigraphic zones are shown for the South Delaware Basin adjacent to the corresponding stratigraphic units. Hatched areas indicate depositional hiatuses.

1.1. Study Area and Fusulinid Biostratigraphy

In this study, we use *Triticites* specimens collected from the Pedregosa (Southeast Arizona and Southwest New Mexico), Orogrande (Southeast New Mexico and West-Northwest Texas), Delaware (Southwest Texas), and Midcontinent (Oklahoma, Kansas, and Nebraska) basins (**Figure 3**). At the time of deposition, these Laurussian basins were near-equatorial epicontinental tropical basins that alternated between open ocean marine, shallow marine, and terrestrial deposition during the Pennsylvanian and Permian on the continent of Laurussia (Koch and Frank, 2011; Henderson et al., 2012). Brachiopod $\delta^{18}O$ indicate that sea surface temperatures (SST) decreased in these basins across the PPB (Flake, 2012; Grossman, 2012) and the Gondwanan ice sheet reached maximum expansion (Montañez et al., 2007). Convergence of northward moving Gondwana with the Marathon-Ouachita-Appalachian arc-trench system in Laurussia and active Marathon-Ouachita crustal shortening were occurring near these basins across the PPB (Ziegler, 2012) impacting the environmental conditions and, potentially, morphological changes within fusulinids, in our studied basins. All four basins were separated from the Paleotethys Ocean to the east by the Marathon-Ouachita-Appalachian arc-trench system and westerly bounded by the Panthalassa Ocean (Ross and Ross, 1985; Ziegler, 2012; Denayer, 2015). Thus, environmental changes in these basins may more closely resemble the Panthalassa Ocean rather than the Paleotethys Ocean. Further, if one of our basins was more restricted or indirectly connected to the Panthalassa Ocean, we might expect inconsistent environmental changes.

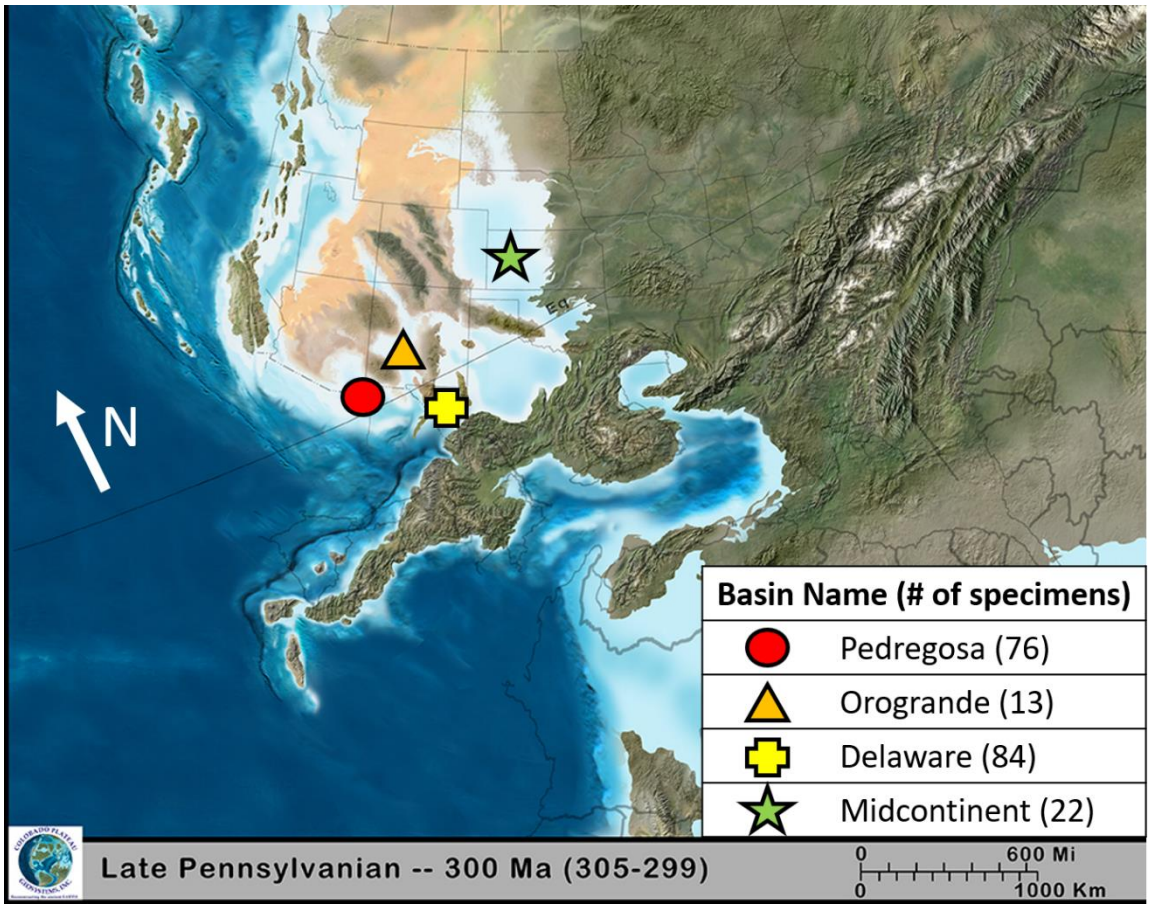

Figure 3: Late Pennsylvanian (300 Ma) paleogeographic map of North America (used with permission © 2013 Colorado Plateau Geosystems Inc.). Symbols indicate location of depositional basins used in this study.

In the Central and Southwestern United States, the base of the Permian that coincides with the Global Standard Stratotype-section and Point (GSSP) in the Russian Urals is defined as the first appearance datum of the "advanced" and "inflated" genera, *Pseudoschwagerina* and *Paraschwagerina*, which both belong to the family Schwagerinidae (Ross, 1963; Koch and Frank, 2011; Zhang and Wang, 2018). However, Wilde (2006) identified a distinct turnover in the genera *Triticites* across the PPB from

Wilde's "*Triticites* Group III" to the first appearance of ventricose, or inflated, *Triticites* (Wilde's "*Triticites* Group IV") (**Figure 2**) and *Schwagerina* that occurs below the GSSP in New Mexico. Wilde (2006) uses this turnover to define the base of the Permian and the informal Newwellian substage, which is synonymous with the Bursumian stage (Lucas et al., 2017b) and the Post-Virgilian sequence (Sabins and Ross, 1963). However, disagreements about the identification of *Triticites* species and, subsequently, the stratigraphic ranges of certain species, has led to age uncertainty in the stratigraphic units crossing the PPB (Lucas et al., 2017b). According to Wilde (2006), no species of *Triticites* occurs above the Newwellian substage. However, Ross (1963, 1965) claims that there are species restricted to the Nealian (Early Wolfcampian) substage, which follows the Newwellian. Wilde (2006) associates these species occurrences in the Nealian substage with sediment reworking, suggested by conglomerates and unconformities (**Figure 2**) and states that *Triticites* species do not occur *in situ* from Nealian rocks. This disagreement about the stratigraphic ranges of *Triticites* species adds confusion to the placement of the PPB within the Central and Southwestern United States (Lucas et al., 2017b). Quantitative morphological identification of *Triticites* species found across the PPB by multiple researchers can help resolve this disagreement.

2. METHODS

2.1. Museum Specimens

Morphological measurements were collected from 195 axial-sectioned specimens of 18 species of *Triticites* spp. housed at the Yale Peabody Museum of Natural History (YPM) Invertebrate Paleontology Collection and the New Mexico Museum of Natural History and Science (NMMNHS) (**Table 1**). All included specimens have preexisting museum catalog numbers (6 digits for YPM and 5 digits for NMMNHS) with the *Triticites* species identification as well as collection data such as locality, lithostratigraphic unit and collector (Dunbar and Condra, 1927; King, 1930, 1937; Dunbar and Skinner, 1937; Ross, 1959, 1963, 1965; Sabins and Ross, 1963; Williams, 1963; Thompson, 1954; Wilde, 2006). All specimens were prepared as a thin section/acetate peel (191) or microdissection cut (4). Thin sections and acetate peels are combined in catalog descriptions because the outcome of both procedures is a thin slice of the fusulinid test. Microdissection cuts involve a bisected test, in which the cut face is glued to a glass slide. Even though both preparation methods reveal the internal morphological structure, thin sections and acetate peels provide a thin slice of the test whereas the microdissection cut preserves the 3-dimensionality of the test.

Table 1: Table of the selected 18 biostratigraphically significant species of *Triticites* in the YPM and NMNMHS collections. For columns with the museum abbreviation, this is the number of specimens for a particular species in the museum's collections that were used in this study. The "Stratigraphic Unit" column shows the stratigraphic unit where each species was found, for the specimens used in this study. The "TOTAL" column shows the total number of specimens for each species used in this study.

Species Name	YPM	NMMNHS	Stratigraphic Unit‡‡	Number of Specimens
T. beedei	10	3	Gaptank Fm, Shawnee Grp, Cisco Grp, Sheridan Canyon Mbr (Horquilla Fm)	13
T. cameratoides	6		Gaptank Fm, Sheridan Canyon Mbr (Horquilla Fm)	6
T. comptus	4	2	Gaptank Fm, Cisco Grp, Sheridan Canyon Mbr (Horquilla Fm)	6
T. creekensis	17		Earp Fm, Sheridan Canyon Mbr (Horquilla Fm)	17
T. cullomensis	16	3	Gaptank Fm, Douglas and Shawnee Grps, Cisco Grp, Sheridan Canyon Mbr (Horquilla Fm)	19
T. elegantoides	7		Gaptank Fm	7
T. gallowayi	9		Gaptank Fm	9
T. inflatus		6	Sheridan Canyon Mbr (Horquilla Fm)	6
T. koschmanni c.f. Leptotriticites pseudokoschmanni*	3	2	Gaptank Fm, Neal Ranch Fm, Sheridan Canyon Mbr (Horquilla Fm)	5
T. meeki	3	3	Earp Fm, Elmdale Fm, Council Grove Grp, Wabaunsee Grp,	6
T. moorei		8	Cisco Grp, Sheridan Canyon Mbr (Horquilla Fm)	8
T. nealensis	2	4	Gaptank Fm, Cisco Grp, Sheridan Canyon Mbr (Horquilla Fm)	6
T. newwellensis		3	Sheridan Canyon Mbr (Horquilla Fm)	3
*T. pinguis**	19	6	Earp Fm, Neal Ranch Fm, Wolfcamp Fm†, Sheridan Canyon Mbr (Horquilla Fm)	25
T. powwowensis	15		Powwow Mbr (Hueco Fm), Wolfcamp Fm	15
T. turgidus	7		Gaptank Fm	7
*T. uddeni**	15		Neal Ranch Fm, Wolfcamp Fm†	15
*T. ventricosus**	19	3	Elmdale Fm, Council Grove Grp, Wabaunsee Grp, Wolfcamp Fm†, Neal Ranch Fm, Gaptank Fm, Admire Grp, Sheridan Canyon Mbr (Horquilla Fm)	22
			Total Used Specimens	195

*****Possible reworking into Nealian sediments, according to Wilde (2006); **†**Found in Wolfcamp Formation in West Texas by R. E. King; **‡‡**Stratigraphic Unit obtained from Wilde (2006), Wahlman (2013), Lucas et al. (2017a) and Yale Peabody Museum Specimen Catalog

All specimens included in analyses have at least 4 well-preserved volutions, or growth stages, a visible proloculus and have an axial orientation with minor spiraling effect permitted. Spiraling effect is a characteristic of oblique sections where the volutions follow a spiral pattern around the proloculus (Dunbar and Skinner, 1937). In addition, specimens had to be free of cracks >10 µm in width and those cracks could not have any displacement in portions of the test younger than the fourth volution. Museum specimen catalog entries indicate whether the specimen was from (5) the Virgilian (late Pennsylvanian), the Newwellian/Bursumian/Post-Virgilian (Wilde, 2002; Ross and Ross, 1994; Sabins and Ross, 1963; respectively) or the Nealian (early Permian) substages, and if it was collected in one of the four targeted depositional basins. Due to the uncertainty concerning whether the lowest Nealian contains reworked Newwellian sediments, these two substages are combined into the Newwellian-Nealian and analyzed together.

We photographed YPM specimens using a Leica MZ16 stereomicroscope with a motorized column, Leica KL2500 and Leica KL1500 illumination with a Leica DMC 4500 camera. If the internal structures were not visible in stereomicroscope, a Leica DM2500P light microscope with a Jenoptik ProgRes CF Scan microscope camera attachment was used at 2.5X and 10X magnification. We photographed NMMNHS specimens using a Nikon SMZ1500 stereomicroscope (2-8X magnification). Magnifications were based on the character measurement needed and varied with the size of the specimen. Higher magnification images (6-8X), which often only included the proloculus and one half of the short axis (**Figure 1**), were chosen for measuring

smaller characters such as the proloculus radius, chamber height, and wall thickness. Lower magnification images (2-4X), which often included the entire test, were chosen for measuring larger characters such as half-length expansion and cross-sectional area.

2.2. Morphological Measurements

We use axial sections for our analysis due to their usefulness in analyzing fusulinid shape change (Groves and Reisdorph, 2009; Shi and Macleod, 2016; Arefifard, 2018). Even though axial sections are prone to inconsistent orientation (Dunbar and Skinner, 1937; Koepnick and Kaesler, 1974), we screened all specimens for consistent orientation to minimize inconsistency. Early morphological studies of fusulinids that used axial sections, focused primarily on proloculus diameter and length and width of entire organism (Dunbar and Condra, 1927; Dunbar and Skinner, 1937), which ignores growth stages of the individual and, thus, ontogenetic variation. More recent studies use proloculus diameter, radius vector, half-length, tunnel width, tunnel angle, wall thickness and chomata height of each volution and account for ontogenetic variation (Ross, 1963; Groves and Reisdorph, 2009). Other studies within the last decade used a simplified measurement scheme focused on the length and width of the entire organism, wall thickness and proloculus diameter, but they measure the characters for each volution, to account for ontogenetic variation (Arefifard, 2018). Landmark techniques and geometric morphometrics of each volution have also been applied to axial section to study ontogenetic shape change (Shi and Macleod, 2016).

Although measurements of proloculus radius, radius vector, and half-length from axial sections commonly accompany taxonomic descriptions (Ross, 1963; Dunbar and

Condra, 1927; Dunbar and Skinner, 1937; Wilde, 2006; and Koepnick and Kaesler, 1974), these measurements of later volutions include the measure of the preceding volution and are, thus, non-independent characters. Non-independent characters can create an artificial covariance and exaggerate the importance of variation in earlier growth stages (Wilkinson, 1995). To prevent some characters from disproportionately influencing the results, we instead measured the inner proloculus radius (PR), chamber height along the radius vector for each volution (CH), half-length expansions for each volution (HLE; the increase in half-length between successive volutions) and wall thicknesses of each volution (WT; thickness of both tectum and keriotheca) (**Figure 4**). Only measurements up to the fourth volution were used in this study.

All axial measurements were standardized by the cross-sectional area of the fourth volution for each specimen to focus the analysis on differences in shape rather than size (Strauss, 2010). The data were transformed with a $\log_{10}$ transformation (*log10* function; R Core Team, 2018), tested for multivariate normality using the Shapiro-Wilk Multivariate Normality Test (*mshapiro.test* function; Jarek, 2012) and were then scaled using the z-score transformation (*scale* function; R Core Team, 2018) to ensure the variance of all measurements contribute equally to the analyses despite difference in scale. Both of these transformations are typically used for morphological studies (Strauss, 2010). All data transformations and statistical analyses were performed in R (version 3.5.2; R Core Team, 2018).

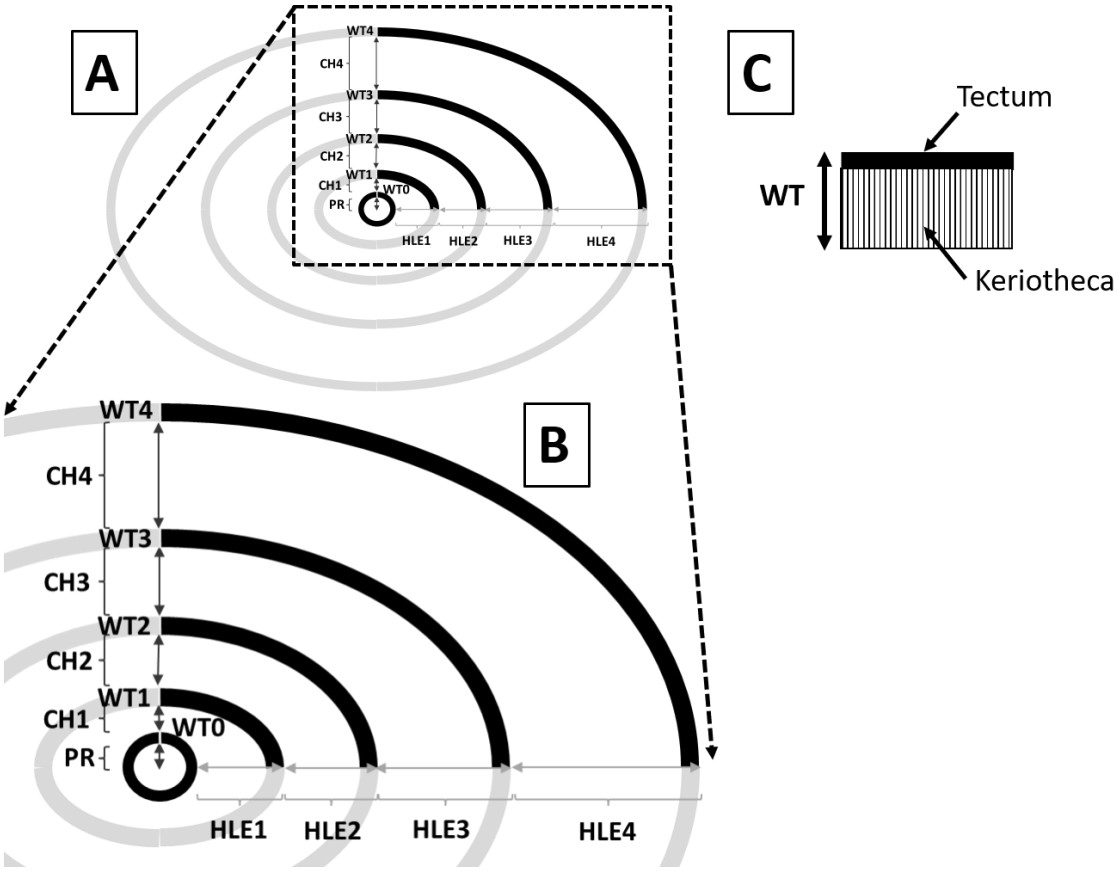

Figure 4: Idealized schematic drawings of Fusulinid foraminiferan volutions with character definitions as seen on an axial section. A) Overall schematic of axial section of fusulinid test; B) Close-up of character definitions on fusulinid test. PR = inner proloculus radius; CH = chamber height along radius vector; HLE = half-length expansion; WT = wall thickness. C) Wall thickness includes the thickness of the tectum and the keriotheca.

2.3. Quantitative Analyses

Studies of fusulinid morphology in the past 20 years have used multivariate ordination analyses such as principal components analysis (PCA) (Shi and Macleod, 2016; Arefifard, 2018), principal coordinates analysis (PCoA) (Arefifard, 2018), non-metric multidimensional scaling (NMDS) (Arefifard, 2018), and canonical variate

analysis (CVA) (Groves and Reisdorph, 2009; Shi and Macleod, 2016). We use a CVA to identify the morphological characters most useful for differentiating among *Triticites* species, a similar linear discriminant analysis (LDA) to determine the morphological difference between the Virgilian and Newwellian-Nealian and a PCA to explore overall morphological variation among specimens.

2.3.1. Multivariate Morphometrics for Species Delimitation

To determine if our morphological characters can be used to consistently differentiate among *Triticites* species, we use a CVA, which is commonly used in morphological studies to visually and quantitatively identify the characters that contribute to the maximum separation of species (Mitteroeker and Bookstein, 2011; Torres-Silva, 2018; Groves and Reisdorph, 2009). A CVA determines the maximum separation between more than two groups, identifies the explanatory characters that best separate those groups (character scalings), and tests if these characters can be used to distinguish between groups through cross-validation ("jack-knifing" or "leave-one-out") analysis. Characters with the most extreme positive and negative scaling values on each axis are the most important to species distinction on that axis. To determine if the 18 *Triticites* species can be differentiated based on the morphological characters mentioned above, a cross-validated CVA was performed using the function *lda* in the R package "MASS" (Venables and Ripley, 2002; R Core Team, 2018) with the species identification as the grouping factor. If species are maximally distinct, then all conspecific specimens will cluster in their own morphospace with little overlap.

2.3.2. Temporal Comparisons of Morphology

Scores on CVA Axis 1 are used to compare morphological differences between the Virgilian and Newwellian-Nealian with a Mann-Whitney U test (*wilcox.test*; R Core Team, 2018). If the median scores of the Virgilian and Newwellian-Nealian are significantly different, morphological differences within *Triticites* between these time bins can be used to identify a morphological shift across the PPB.

Additionally, we performed a linear discriminant analysis (LDA) to focus on any morphological changes that occur within *Triticites* across the PPB. An LDA is similar to a CVA but only differentiates between two groups. A cross-validated LDA was performed using the same function *lda* in the R package "MASS" (Venables and Ripley, 2002) with time bin (Virgilian or Newwellian-Nealian) as the grouping factor.

As with the CVA, we test whether the LDA scores for specimens are significantly different between the Virgilian and Newwellian-Nealian using a Mann-Whitney U test. We then use the scalings of the morphological characters to define the primary characters that exhibit change between the Virgilian and Newwellian-Nealian. We further subset the LDA by geologic basin and tested for significant differences between median LDA scores for specimens in the Virgilian and Newwellian-Nealian for each basin, using a Mann-Whitney U test, to test the hypothesis that the morphological changes are consistent between basins and not driven by changes in a single basin.

2.3.3. Total Morphological Variation Within *Triticites*

Principal components analysis (PCA) has been used in several morphometric studies (Shi and Macleod, 2016; Arefifard, 2018; Torres-Silva et al, 2018) to examine

the variation among specimens without apriori categorization. We use this more exploratory ordination to examine our data and test whether the morphological changes that we identify using the CVA and LDA are independent of species or age categorization. The PCA was performed using the function *prcomp* in the R package "stats" (R Core Team, 2018). PCA scores of specimens are subset by Virgilian or Newwellian-Nealian and basins for a comparison using a Mann-Whitney U test to verify the CVA and LDA results.

3. RESULTS

3.1. Species-Based CVA

CVA Axes 1, 2 and 3 summarize 50.22%, 16.58% and 15.41% of the morphological variation, respectively. Even though there are 11 more axes of variation, each subsequent axis summarizes less than 10% of the variation and are not discussed further. On CVA Axis 1, species with the most positive scores include *T. creekensis*, *T. inflatus*, and *T. pinguis* and species with the most negative scores are *T. comptus*, *T. moorei*, *T. nealensis*, and *T. powwowensis* (**Figure 5**). Specimens with the most positive scores on CVA Axis 1 correspond to higher values of wall thickness of the proloculus (WT0), proloculus radius (PR), half-length expansion of the second volution (HLE2), and wall thickness of the first volution (WT1), which have the most positive character scalings (**Table 2**). Specimens with the most negative scores correspond to higher values of half-length expansion of the third and fourth volutions (HLE3, HLE4), wall thickness of the second volution (WT2), and half-length expansion of the first volution (HLE1), which have the most negative character scalings (**Table 2**). On CVA Axis 2, *T. powwowensis* and *T. uddeni* have the most positive scores whereas *T. comptus*, *T. koschmanni*, and *T. turgidus* have the most negative scores (**Figure 5A**). Specimens with the most positive scores on CVA Axis 2 correspond to higher values of wall thickness of the fourth volution (WT4), chamber height of the first volution (CH1), proloculus radius (PR), and wall thickness of the second volution (WT2), which have the most positive character scalings (**Table 2**). Specimens with the most negative scores correspond to

higher values of half-length expansion of the second volution (HLE2), wall thickness of the proloculus (WT0), half-length expansion of the first volution (HLE1), and chamber height of the third volution (CH3), which have the most negative character scalings (**Table 2**). On CVA Axis 3, *T. comptus, T. creekensis,* and *T. newwellensis* have the most positive scores, while *T. elegantoides, T. moorei*, and *T. powwowensis* have the most negative scores (**Figure 5B).** Specimens with the most positive scores on CVA Axis 3 correspond to higher values of wall thickness of the proloculus (WT0), half-length expansion of the third and fourth volutions (HLE3, HLE4), and wall thickness of the first volution (WT1), which have the most positive character scalings (**Table 2**). Specimens with the most negative scores correspond to higher values of chamber height of the fourth volution (CH4), chamber height of the third volution (CH3), wall thickness of the fourth volution (WT4), and wall thickness of the second volution (WT2), which have the most negative character scalings (**Table 2**). Specimens from each basin are distributed evenly in ordination space, with the exception of the Orogrande Basin, which only had specimens from the Newwellian-Nealian (**Figure 5E-F**).

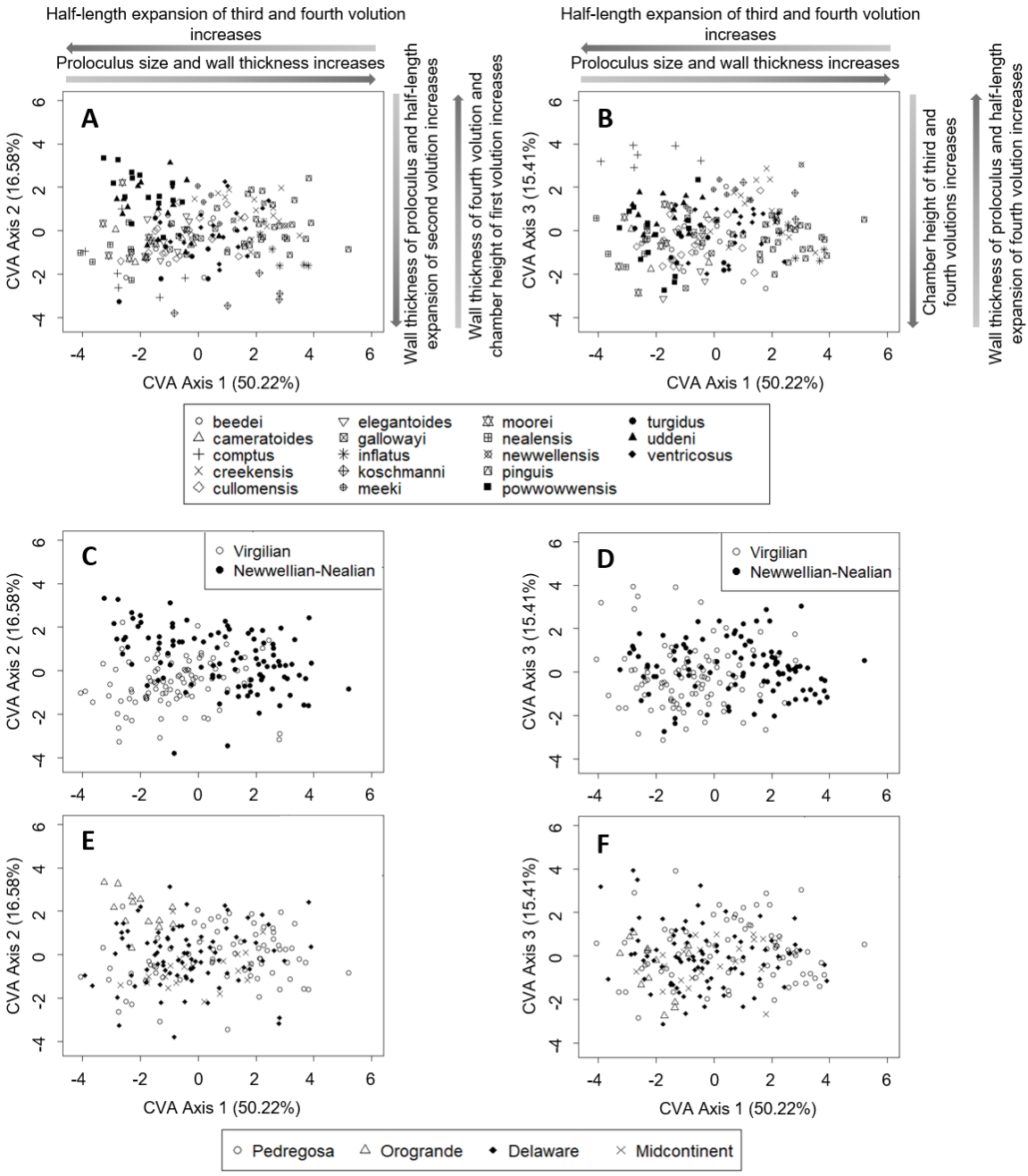

Figure 5: Specimen scores from CVA Axes 1 and 2 (A, C, and E) and CVA Axes 1 and 3 (B, D, and F) showing specimen distribution in the morphospace. A-B) symbols correspond to species (legend below plots); C-D) symbols correspond to time bin; E-F) symbols correspond to basin (legend below plots). Gradational arrows on A and B indicate the direction in which the noted character measurements are increasing on each axis. Gradational arrows on A are the same on C and E. Gradational arrows on B are the same on D and F.

Table 2: Character scalings for the first 3 axes of the species-based CVA and Stratigraphic age-based LDA and character loadings for the first 2 axes of the PCA. Bold scalings/loadings are the most positive and the most negative along each axis. PR = inner proloculus radius; CH = chamber height along radius vector; HLE = half-length expansion; WT = wall thickness. Numbers on character abbreviations correspond to the volution or growth stage number.

Characters	CVA Axis 1	CVA Axis 2	CVA Axis 3	LDA	PCA Axis 1	PCA Axis 2
PR	**0.468**	**0.239**	0.354	**0.413**	-0.253	**-0.281**
CH1	-0.100	**0.240**	0.247	**0.259**	-0.285	-0.117
CH2	0.281	-0.270	0.141	0.029	-0.290	-0.121
CH3	-0.065	**-0.396**	**-0.995**	**-0.876**	-0.302	0.064
CH4	0.270	-0.364	**-1.325**	0.157	-0.285	**0.250**
HLE1	**-0.113**	**-0.469**	-0.071	**-0.397**	-0.192	-0.056
HLE2	**0.443**	**-0.617**	-0.091	**-0.391**	-0.277	**0.143**
HLE3	**-0.529**	0.007	**0.700**	-0.191	-0.253	**0.432**
HLE4	**-1.800**	0.031	**0.876**	**-0.484**	-0.196	**0.637**
WT0	**0.498**	**-0.528**	**0.911**	**0.374**	-0.272	**-0.237**
WT1	**0.313**	-0.105	**0.571**	**0.239**	-0.258	**-0.309**
WT2	**-0.274**	**0.224**	**-0.236**	-0.089	-0.282	**-0.226**
WT3	-0.102	-0.092	0.028	-0.389	-0.284	-0.069
WT4	0.025	**0.768**	**-0.839**	0.216	-0.287	0.046

While there is considerable congeneric overlap on the first three axes, some species have a more restricted morphospace and are separate from some, but not all, species on one or two axes. The median CVA Axis 1 score of *T. uddeni* is significantly different from the median score of *T. pinguis* ($U = 1$, $p<0.001$), *T. creekensis*, ($U = 3$, $p<0.001$), and *T. inflatus* ($U = 0$, $p<0.001$). The median CVA Axis 1 score of *T.*

nealensis is also significantly different from the median scores of *T. pinguis* (U = 0, p<0.001), *T. creekensis* (U = 0, p<0.001), and *T. inflatus* (U = 0, p=0.002). The median CVA Axis 1 score of *T. comptus* is also significantly different from the median scores of *T. pinguis* (U = 0, p<0.001), *T. creekensis* (U = 0, p<0.001), and *T. inflatus* (U = 0, p=0.002). On CVA Axis 2, *T. koschmanni* differs from all other species due to its relatively large half-length expansion of the second volution (HLE2) and relatively large wall thickness of the proloculus (WT0), which have the most negative character scalings on CVA Axis 2. *T. comptus* differs from all species on CVA Axis 3 due to its relatively large half-length expansions of the third and fourth volutions (HLE3 and HLE4), which have the highest positive scalings on CVA Axis 3.

The cross-validated CVA correctly predicted species identification for approximately 27% of specimens. Incorrect predictions occurred more often within the same time bin rather than across time bins. Of the 142 specimens that were not identified as their assigned species, approximately 77% were identified as a species found within the same time bin as the specimen's assigned species. The median CVA Axis 1 score for the Virgilian (median = -0.916; IQR = -1.767 to 0.053) is significantly lower than for the Newwellian-Nealian (median = 1.021; IQR = -0.880 to 2.231) according to a Mann-Whitney U test (U = 2549; p<0.001) (**Figure 5C-D and 6A**). Similarly, the median CVA Axis 2 score for the Virgilian (median = -0.564; IQR = -1.195 to 0.085) is significantly lower than for the Newwellian-Nealian (median = 0.450; IQR = -0.366 to 1.507) according to a Mann-Whitney U test (U = 2401; p<0.001) (**Figure 5C**). Species with the most positive scores on CVA Axis 1 or CVA Axis 2 or both, including *T.*

creekensis, *T. inflatus*, *T. meeki*, *T. newwellensis*, *T. pinguis*, and *T. powwowensis*, were species that were found almost exclusively in the Newwellian-Nealian (**Figure 5A**).

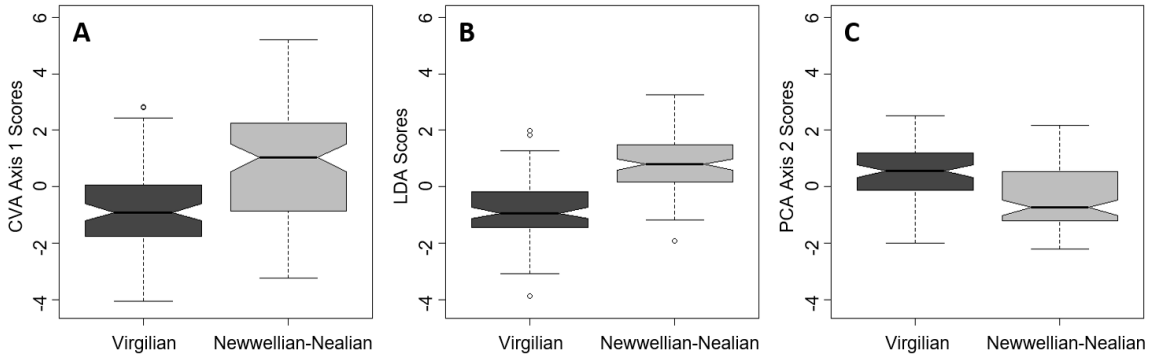

Figure 6: A) CVA Axis 1 scores for Virgilian and Newwellian-Nealian. B) LDA scores for Virgilian and Newwellian-Nealian. C) PCA Axis 2 scores for Virgilian and Newwellian-Nealian. Shaded box represents the interquartile range (IQR). Lower box bound represents the 25th percentile (Q1) and the upper box bound represents the 75th percentile (Q3). Lower whisker represents the minimum values outside the IQR (Q1-1.5*IQR). Upper whisker represents the maximum values outside the IQR (Q3+1.5*IQR). Circles outside whiskers are the outliers. Thick middle line represents the median score. Notch represents 95% confidence around the median.

Even though the species mentioned above have scores restricted to either the positive or negative end of a CVA Axis, some species, including *T. beedei*, *T. cullomensis*, *T. gallowayi* and *T. ventricosus*, have a wide range of scores always in the -2 to 2 score range on the all first three axes. Only two of these species, *T. cullomensis* and *T. ventricosus* are species that are found in both the Virgilian and Newwellian-Nealian. While *T. ventricosus* has 10 Virgilian specimens and 12 Newwellian-Nealian specimens, *T. cullomensis* has 17 Virgilian specimens and only 2 Newwellian-Nealian

specimens. Virgilian and Newwellian-Nealian specimens of *T. cullomensis* were not significantly different according to a Mann-Whitney U test on CVA Axis 1 (U = 8, p=0.292), CVA Axis 2 (U = 14, p=0.749), and CVA Axis 3 (U = 25, p=0.351). Virgilian and Newwellian-Nealian specimens of *T. ventricosus* were not significantly different according to a Mann-Whitney U test on CVA Axis 1 (U = 68, p=0.628), CVA Axis 2 (U = 53, p=0.674), and CVA Axis 3 (U = 76, p=0.314). The other species found in both the Virgilian and Newwellian-Nealian, *T. koschmanni*, does not exhibit this restricted range of scores, which seems to be restricted to the most negative values on CVA Axis 2. However, Virgilian and Newwellian-Nealian specimens of *T. koschmanni* were still not significantly different according to a Mann-Whitney U test on CVA Axis 1 (U = 6, p=0.200), CVA Axis 2 (U = 4, p=0.800), and CVA Axis 3 (U = 2, p=0.800).

3.2. Temporally-Based LDA

The cross-validated LDA correctly predicted specimen placement into the Virgilian or Newwellian-Nealian for approximately 77% of specimens. The largest positive character scalings are proloculus radius (PR), wall thickness of the proloculus (WT0), chamber height of the first volution (CH1), and wall thickness of the first volution (WT1) and the largest negative character scalings are chamber height of the third volution (CH3) and half-length expansion of the first, second, fourth volutions (HLE1, HLE2, HLE4) (**Table 2**). The median LDA score for the Virgilian (median = -0.937; IQR= -1.454 to -0.193) is significantly lower than for the Newwellian-Nealian (median = 0.786; IQR = 0.177 to 1.465) according to a Mann-Whitney U test (U = 1185; p<<0.001) (**Figure 6B**).

LDA scores are also significantly different between the Virgilian and Newwellian-Nealian in each studied basin (**Figure 7, Table 3**). Since there is no data from the Virgilian in the Orogrande Basin, no Mann-Whitney U test was conducted for this basin. The median LDA score for the Virgilian was significantly smaller than for the Newwellian-Nealian in the Pedregosa, Delaware and Midcontinent basins (**Table 3**). The median LDA scores for the Pedregosa basin in the Virgilian and Newwellian-Nealian have the largest difference (**Table 3**) and the interquartile ranges of each time bin do not overlap (**Figure 7**). The median LDA scores of the Virgilian and Newwellian-Nealian for the Delaware and the Midcontinent basin have a smaller difference than the Pedregosa (**Figure 7, Table 3).**

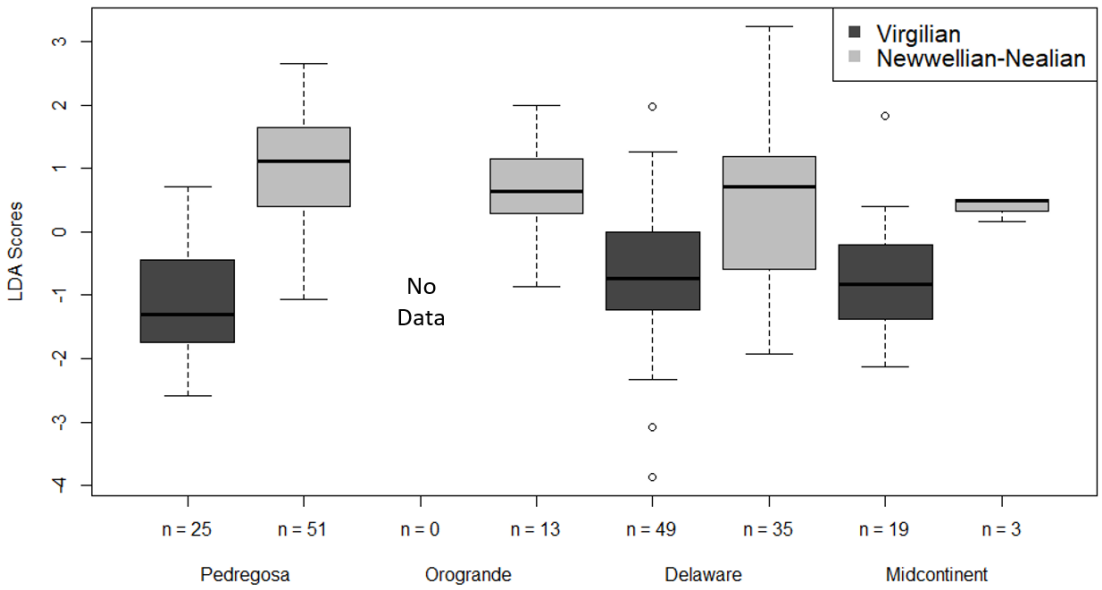

Figure 7: Stratigraphic age-based LDA scores of each studied basin (Pedregosa, Orogrande, Delaware, and Midcontinent) for the Virgilian and Newwellian-Nealian (n = number of specimens). Shaded box represents the interquartile range (IQR). Lower box bound represents the 25th percentile (Q1) and the upper box bound represents the 75th percentile (Q3). Lower whisker represents the minimum values outside the IQR (Q1-1.5*IQR). Upper whisker represents the maximum values outside the IQR (Q3+1.5*IQR). Circles outside whiskers are the outliers. Thick middle line represents the median score.

Table 3: Sample size, median, interquartile range (IQR), and Mann-Whitney U test results for stratigraphic age-based LDA scores in each time bin for each basin.

Basin Name	Time Bin	Sample Size	Median	IQR	Mann-Whitney Results	
					U	p
Pedregosa	Virgilian	25	-1.306	-1.750 to -0.438	48	< 0.001
	Newwellian-Nealian	51	1.113	0.393 to 1.639		
Orogrande	Virgilian	0	--	--	--	--
	Newwellian-Nealian	13	0.640	0.280 to 1.150		
Delaware	Virgilian	49	-0.742	-1.231 to -0.004	384	< 0.001
	Newwellian-Nealian	35	0.718	-0.592 to 1.182		
Midcontinent	Virgilian	19	-0.837	-1.375 to -0.201	4	0.014
	Newwellian-Nealian	3	0.498	0.331 to 0.506		

3.3. Total Morphological Variation

PCA Axis 1 summarizes 65.33% of the morphological variation and PCA Axis 2 summarizes 9.64% of the morphological variance (**Figure 8**). The remaining 13 axes each summarized less than 10% of the variance and are not discussed further. On PCA Axis 1, all character loadings are negative and between -0.302 and -0.192 (**Table 2**). Species with the most positive scores on PCA Axis 1 include *T. comptus*, *T. powwowensis*, *T. uddeni*, and *T. ventricosus*, while species with the most negative scores include *T. beedei*, *T. cameratoides*, *T. creekensis*, *T. nealensis*, and *T. turgidus* (**Figure 8A**). On PCA Axis 2, the most positive character loadings include half-length expansion of the second, third, and fourth volutions (HLE2, HLE3, HLE4) and chamber height of the fourth volution (CH4), while those with the most negative character loadings include proloculus radius (PR), wall thickness of the proloculus (WT0) and wall thickness of the first and second volutions (WT1, WT2) (**Table 2**). Species with the most positive scores on PCA Axis 2 include *T. pinguis*, *T. inflatus*, *T. koschmanni*, *T. creekensis*, and *T. newwellensis*, while species with the most negative scores include *T. moorei*, *T. comptus*, *T. nealensis*, *T. cullomensis*, and *T. uddeni* (**Figure 8A**).

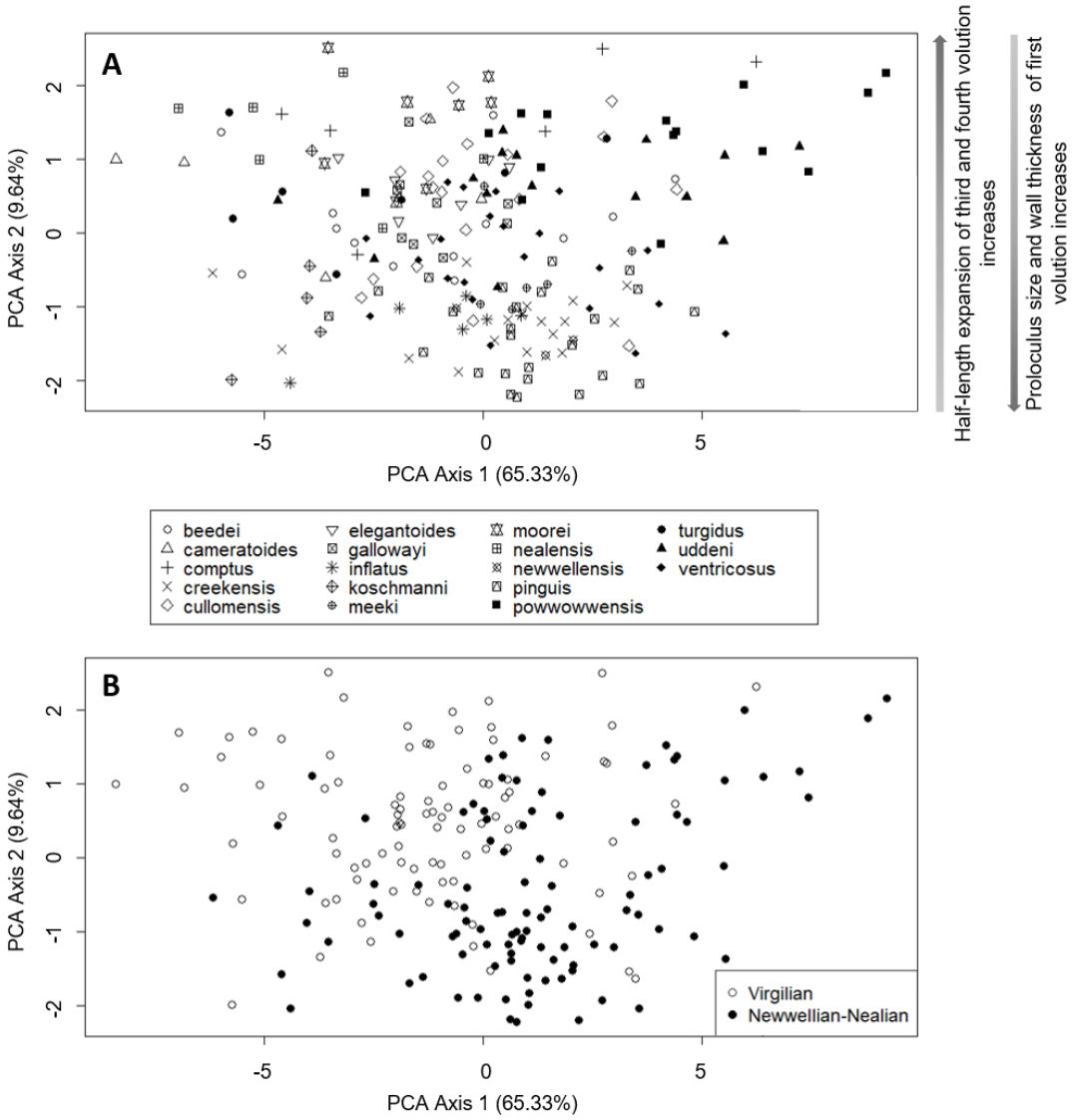

Figure 8: Specimen scores from PCA Axes 1 and 2 showing specimen distribution in the morphospace. A) symbols correspond to species (legend below plot); B) symbols correspond to time bin; C) symbols correspond to basin. Gradational arrows on A indicate the direction in which the noted character measurements are increasing on PCA Axis 2 and are the same for B and C.

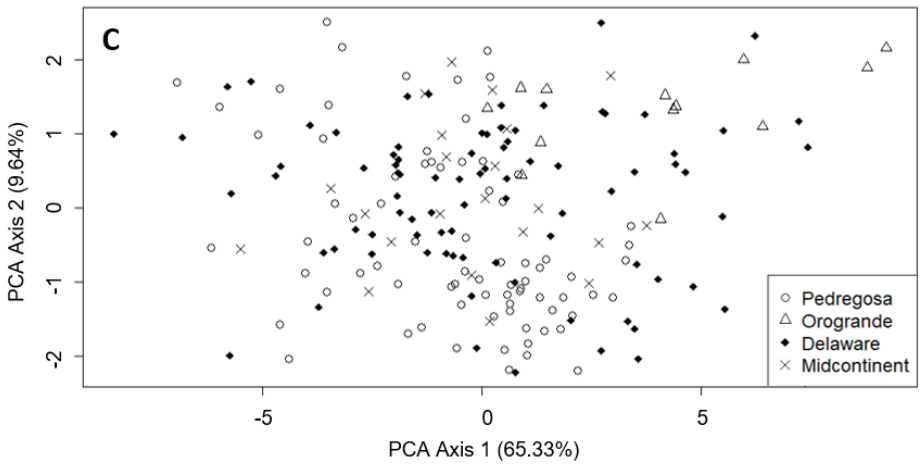

Figure 8 Continued

The PCA shows the same congeneric overlap as the CVA where some species have a more restricted morphospace and are separate from some, but not all, species on one or two axes (**Figure 8A**). As in the CVA, the median PCA Axis 2 score of *T. uddeni* is significantly different from the median scores of *T. pinguis* ($U = 371$; $p<0.001$), *T. creekensis* ($U = 252$; $p<0.001$), and *T. inflatus* ($U = 90$; $p<0.001$). The median PCA Axis 2 score of *T. nealensis* is also significantly different from the median scores of *T. pinguis* ($U = 150$; $p<0.001$), *T. creekensis* ($U = 102$; $p<0.001$), and *T. inflatus* ($U = 36$; $p=0.002$). The median PCA Axis 2 score of *T. comptus* is significantly different from the median scores of *T. pinguis* ($U = 150$; $p<0.001$), *T. creekensis* ($U = 102$; $p<0.001$), and *T. inflatus* ($U = 36$; $p=0.002$).

Median scores for Virgilian and Newwellian-Nealian specimens are significantly different on both PCA Axis 1 ($U = 2347$, $p<0.001$) and PCA Axis 2 ($U = 6901$,

p<0.001). On PCA Axis 1, Virgilian specimens have the most negative scores, while on PCA Axis 2, they have the most positive scores (**Figure 8B**). On PCA Axis 1, Newwellian-Nealian specimens have the most positive scores, while on PCA Axis 2, they have the most negative scores (**Figure 8B**). The temporal difference seen on PCA Axis 2 is consistent among basins (**Table 4**). Specimens from each basin are distributed evenly in ordination space, with the exception of the Orogrande Basin, which only had specimens from the Newwellian-Nealian (**Figure 8C**).

Table 4: Sample size, median, interquartile range (IQR), and Mann-Whitney U test results for PCA Axis 2 scores in each time bin for each basin.

Basin Name	Time Bin	Sample Size	Median	IQR	Mann-Whitney Results	
					U	p
Pedregosa	Virgilian	25	0.939	0.418 to 1.688	1229	< 0.001
	Newwellian-Nealian	51	-1.134	-1.522 to -0.797		
Orogrande	Virgilian	0	--	--	--	--
	Newwellian-Nealian	13	1.372	1.093 to 1.613		
Delaware	Virgilian	49	0.447	-0.155 to 0.991	1059	0.068
	Newwellian-Nealian	35	-0.118	-0.867 to 0.678		
Midcontinent	Virgilian	19	0.119	-0.520 to 1.013	34	0.651
	Newwellian-Nealian	3	-0.239	-0.285 to -0.126		

4. DISCUSSION

4.1. Species Differentiation Among *Triticites* Species

The CVA showed that specimens of a given species occupy a similar morphospace, but congenerics overlap considerably in morphospace (**Figure 6**) and species prediction accuracy was only 27%. A similar congeneric overlap was observed in specimens of the fusulinid genus, *Beedeina*, which is very similar in morphology to *Triticites* (BouDagher-Fadel, 2018), from middle Pennsylvanian rocks in the Ardmore Basin of southern Oklahoma (Groves and Reisdorph, 2009). For a few of the *Beedeina* species, this observation was related to an evolutionary relationship among congeneric species such that the more derived species exhibited small amounts of overlap, while the less derived species exhibited more overlap (Groves and Reisdorph, 2009). The characters that are most important for *Beedeina* species differentiation are the diameter of the proloculus, thickness of tectum and diaphanotheca of the first volution, half-length of the first volution, half-length of the sixth volution and radius vector of the fifth volution (Groves and Reisdorph, 2009). These findings are similar to the morphological differences among *Triticites* species where the largest positive character scalings on CVA Axis 1 are wall thickness and radius of the proloculus (WT0, PR), half-length expansion of the second volution (HLE2), and wall thickness of the first volution (WT1). Elements of half-length that are important on our CVA Axis 1 and CVA Axis 3 and elements of radius vector that are important on our CVA Axis 2 and CVA Axis 3 (**Table 2**), are also similar to the taxonomically important characters that differentiate among

Beedeina (Groves and Reisdorph, 2009). Half-length expansion measures have strong negative scalings on our CVA Axis 1 and strong positive scalings on our CVA Axis 3, while chamber height measures have strong negative scalings on our CVA Axis 3 (**Table 2**).

Morphological changes within *Triticites* species primarily reflect the size of the proloculus and the extent of elongation of the test. Species that are restricted to the negative end of CVA Axis 1 (*T. uddeni*, *T. nealensis*, and *T. comptus*; **Figure 5**) all have relatively large half-length expansions of the third and fourth volutions and relatively small proloculi, which are indicative of a long fusiform or "more elongated" test with small proloculi. The species restricted to the positive end of CVA Axis 1 (*T. pinguis*, *T. creekensis*, and *T. inflatus*; **Figure 5**) all have relatively large proloculi and relatively small half-length expansions of the third and fourth volutions, which are indicative of a short fusiform or "less elongated" test with large proloculi. Species with highly variable morphology, such as *T. ventricosus*, have a proloculus relatively larger than those species with the most negative CVA Axis 1 scores, but not as large as those species with the most positive CVA Axis 1 scores. Similarly, *T. ventricosus* is not as elongate as the species with the most negative CVA Axis 1 scores, but not as short as the species with the most positive CVA Axis 1 scores. These distinct species morphologies quantified here are very similar to qualitative observations found by comparing depositional facies of the late Pennsylvanian Gaptank Formation in West Texas using *Triticites* species (Ross, 1965). In the Pennsylvanian Gaptank study, deep water facies were characterized by elongate and irregular tests and shallow shelf facies were characterized by thickly

(i.e. long) fusiform tests, while the shelf edge facies were characterized as a mixture of the shallow and deep morphologies (Ross, 1965). Thus, species with long fusiform tests and negative CVA Axis 1 scores may indicate a deeper water facies, while species with short fusiform tests and positive CVA Axis 1 scores may indicate a shallow water facies (**Figure 5**).

4.2. Temporal Patterns in Morphology

Despite overall poor species differentiation, CVA Axis 1 records a temporal morphological shift associated with stratigraphic age. There is a significant morphological change across the Virgilian and Newwellian-Nealian transition shown by both CVA Axis 1 and LDA scores. Virgilian specimens have larger half-length expansions (HLE) relative to the size of the organism than Newwellian-Nealian specimens. Newwellian-Nealian specimens have a larger proloculus (PR) and proloculus wall thickness (WT0) relative to the size of the organism than Virgilian specimens, according to both the CVA and LDA (**Table 2**). All characters that are relatively larger in the Newwellian-Nealian represent the embryonic and early juvenile stages of the fusulinid (BouDagher-Fadel, 2018; Groves and Reisdorph, 2009). All characters that are relatively larger in the Virgilian represent growth in later life stages of the fusulinid (BouDagher-Fadel, 2018; Groves and Reisdorph, 2009).

The PCA showed that, regardless of ordination method, *Triticites* have significant morphological differences across the PPB. The common directionality of character loadings on PCA Axis 1 (**Table 2**), indicates that despite size standardization, the PCA still shows that size covaries with shape change. While PCA Axis 2

summarizes less morphological variation, the character loadings distinguish ontogenetically younger parts of the test from ontogenetically older parts of the test that consistent with CVA Axis 1 and the LDA (**Table 2**). This indicates that this morphological change can be identified regardless of prior knowledge of species classification or stratigraphic age.

The proloculus is the first ontogenetic stage and reflects the size of the embryo in foraminifera (Thompson, 1948; Ross, 1972; Groves and Reisdorph, 2009; BouDagher-Fadel, 2018). In modern foraminifera, the size of the offspring produced by the mature adult is dependent on the size of the reproducing adult (Charnov and Ernest, 2006; Caval-Holme et al., 2013), reproductive strategy, and physiological and ecological limitations (Charnov and Ernest, 2006). Even though offspring produced by asexual reproduction will be larger than offspring produced by sexual reproduction (Beavington-Penney and Racey, 2004), a large adult, regardless of the reproduction type will produce a large offspring (Beavington-Penney and Racey, 2004; Charnov and Ernest, 2006). Large proloculi suggest the parent made a greater investment in the embryo indicative of a K-selected reproductive strategy (Caval-Holme et al., 2013). K-selected reproduction requires the parent to ration resources over long periods of time due to unfavorable conditions resulting in slow growth and maturity at larger sizes (Bradshaw, 1957; Hottinger, 1982; Beavington-Penney and Racey, 2004), which result in large offspring at the time of reproduction. K-selected reproduction is commonly associated with asexual reproduction because both suggest the parent's investment in the survival of the embryo

during unfavorable conditions (Hottinger, 1982; Harney et al., 1998; Beavington-Penney and Racey, 2004).

Since large proloculus size appears to reflect asexual reproduction due to unfavorable conditions, fusulinids may be responding to loss of habitat and a change in temperature and salinity. In modern benthic foraminifera, proloculus size increases when there is increased nutrient input due to water erosion of continents and/or deposition of dust in the surface waters (Nigam and Rao, 1987; Schmidt et al., 2018; Keating-Bitoni and Payne, 2018), decreased sea surface temperature and salinity (Nigam and Rao, 1987), and subsequently, increased surface water productivity such as algal blooms (Hottinger, 1982). This shift from microspheric to megalospheric in modern foraminifera is commonly associated with change from sexual to asexual reproduction (Nigam and Rao, 1987; Beavington-Penney and Racey, 2004). Further, during glacial periods, increased sediment and freshwater input from the continents to the ocean would promote these algal blooms and facilitate this change in reproductive strategy (Soreghan et al., 2015). These high-nutrient conditions appear to reflect a K-selected asexual reproductive strategy (Hottinger, 1982; Lipps, 1982). However, Harney et al. (1998) suggests that asexual reproduction is indicative of the colonization of marginal and/or new habitats and unfavorable conditions. High nutrient conditions in the modern ocean are commonly associated with increased freshwater input, which would decrease the salinity of the surface waters, producing unfavorable conditions for the foraminifera (Nigam and Rao, 1987). During the Pennsylvanian-Permian transition, the Gondwanan ice sheet reached its maximum expansion and the oceans saw the lowest CO_2 and tropical sea surface

temperatures (Montañez et al., 2007; Vachard et al., 2010). However, latest Pennsylvanian and earliest Permian oceans had one of the highest salinities in the Phanerozoic (Hay et al., 2006), which could be unfavorable for fusulinid reproduction. Even though glacial ice was already present during the late Pennsylvanian (Grossman, 2012), increased continental ice production would result in a drop in relative sea level, increased weathering, and an increased nutrient supply to the oceans and a resulting increase in productivity (Soreghan et al., 2015). This drop in sea level, as seen across the PPB, would have decreased the inner and middle platform area suitable for Schwagerinoidea (Ross, 1972; Groves and Wang, 2013), which could also be unfavorable for fusulinid reproduction. Paleosols and plant beds, which are indicative of subaerial exposure, have been found in early Wolfcampian age sediments in our studied basins (King, 1930; Olszewski and Patzkowsky, 2003; DiMichele et al., 2006; Koch and Frank, 2011; Lucas et al., 2017b). Certain characteristics of these Wolfcampian paleosols and plant beds indicate seasonally lower precipitation and lower water table, which is characteristic of a seasonally semi-arid to arid climate and in contrast to the ever-wet and seasonal humid climate of the Virgilian (DiMichele et al., 2006). In addition, these arid climate indicators are found during eustatic lows in sea level associated with glacial cyclicity (Olszewski and Patzkowsky, 2003). The morphological change observed in our specimens across the PPB could indicate a shift to K-selected asexual reproduction in response to lower sea surface temperatures, high nutrient levels, high salinity, and decreased shelf area suitable for *Triticites* due to lower sea level.

In Schwagerinid fusulinids, the presence of the keriothecal wall type is associated with the acquisition of photosymbionts (BouDagher-Fadel, 2018). Half-length expansion reflects elongation or shortening of the entire test during later growth stages in response to changing environmental conditions to better accommodate these photosymbionts. Fusiform or elongate tests with large surface area to volume ratios allow for more photosymbionts to be incorporated into the keriotheca and thin walls allow greater light penetration to accommodate the symbionts in the deep water (Hohenegger, 2009; Groves et al., 2012; Groves and Wang, 2013). In contrast, subspherical to spherical tests with small surface area and thick walls reduce the amount of light penetration, protecting the symbionts from harmful ultraviolet light in shallow water (Hohenegger, 2009; Groves and Wang, 2013). Species with the most negative scores on CVA Axis 1 and the LDA are associated with the Virgilian and species with the most positive scores on CVA Axis 1 and the LDA are associated with the Newwellian-Nealian. Virgilian species have longer fusiform tests, which are indicative of a deeper water environment, while Newwellian-Nealian species have shorter fusiform tests, which are indicative of a shallow water environment. This could be in response to a shift from a deep to shallow water environment across the PPB indicated by the drop in sea level across the boundary (Ross and Ross, 1995).

The difference in median LDA scores between the Virgilian and Newwellian-Nealian become larger from the east to the west (**Figure 7, Table 3**). The magnitude of the differences between median PCA Axis 2 scores in the Virgilian and Newwellian-Nealian for each basin is similar to those of the LDA scores (**Table 3 and 4**). For both

ordinations, the Pedregosa basin shows the largest difference between the Virgilian and Newwellian-Nealian, while the Delaware and Midcontinent basins show the smallest difference (**Figure 7, Table 3 and 4**). While the Pedregosa basin has a larger difference between the Virgilian and Newwellian -Nealian than that of the Delaware basin, this cannot be attributed to differences in sample sizes because the Pedregosa and Delaware basins have similar sample sizes (76 and 84 specimens, respectively; **Figure 3**). However, even though the difference between Virgilian and Newwellian-Nealian mean scores of the Midcontinent is similar to that of the Delaware basin, the high p (low significance of difference) for the Midcontinent basin is most likely due to the small sample size of the Newwellian-Nealian for that basin (**Table 3 and 4**). A similar gradient in morphological distinctiveness, associated with depositional facies, was also seen in multiple fusulinid families from Virgilian sections from Kansas that related to water depth (Groves et al., 2012). At the Virgilian Kansas localities with relatively more deep-water shale, indicating localities farther from shore, median test surface area to volume ratios of the transgressive sequence were smaller than those of the regressive sequence. At the Virgilian Kansas locality with relatively less deep-water shale, indicating a locality closer to shore, median test surface area to volume ratios of the transgressive sequence were not much different from those of the regressive sequence. Another gradient was seen in carbon and oxygen isotope ratios in mid-late Carboniferous North America relating to an increase in salinity from east to west due to less terrestrial freshwater input (Flake, 2012). Therefore, the temporal morphological shift will not be as pronounced if the basin is closer to the shore and has less saline

conditions. In our studied basins, going from east to west, the center of the continent is farther away and basins are becoming deeper and more saline when closer to the Panthalassa Ocean. These deeper basins would record a wider range of water depths and have a higher salinity than shallow, near-shore basins.

4.3. Biostratigraphic Implications

In the context of biostratigraphy, these morphological changes are useful for identifying the PPB in the Central and Southwestern United States. Here we quantify the previously qualitative observations of an increase in inflation in fusulinids across the boundary (King, 1930, 1937; Ross, 1963; Wilde, 2006; Lucas et al., 2017b). There is a clear change from longer fusiform tests with small proloculi in the Virgilian to short fusiform tests with large proloculi in the Newwellian-Nealian. However, even though these changes are likely responding to global sea level fall, the morphology and oceanography of the specific basin under study could influence other conditions such as nutrient levels, salinity and temperature. Therefore, this morphological change in *Triticites* may not be as distinct in all basins globally. For the Central and Southwestern United States, this change, originally noted by previous biostratigraphers (King, 1930, 1937; Ross, 1963, 1965, 1972; Wilde, 2006; Lucas et al., 2017b), is quantifiable.

Across the PPB, some species are morphologically distinct from each other, such as *T. comptus* (Virgilian) and *T. pinguis* (Newwellian-Nealian), such that their presence or absence could be used as a biostratigraphic indicator. However, we have identified a morphological shift that is shared by the genus as a whole and not by an individual species. Therefore, this shift occurs in all members of the genus *Triticites* and

does not depend on species-level identifications. This morphological shift is useful for biostratigraphy because it does not depend on species identification or prior stratigraphic age association and can be observed by a non-expert. However, while this morphological shift is restricted to the 18 species within *Triticites* used in this study, similar morphological responses to changing environments could be seen in other fusulinid groups as well as other foraminiferan groups in other time periods. This is because many different foraminifera can respond, morphologically, in the same way in many different time periods depending on environmental conditions.

5. CONCLUSIONS

Triticites species identification and distinction is poor and there is considerable overlap in congeneric morphospace. However, while individual species are difficult to distinguish, certain morphologies can be distinguished and correlated with age. Late Pennsylvanian (Virgilian) morphologies have small proloculi and are more elongated along the long axis in later growth stages, while early Permian (Newwellian-Nealian) morphologies have large proloculi and are wider along the short axis in later growth stages. This change in proloculus size appears to reflect a shift in reproductive strategy from deep water, r-selected sexual reproduction to shallow water, K-selected asexual reproduction indicative of stressful conditions. Modern benthic foraminifera exhibit this strategy shift in low temperature, low salinity, and high nutrient conditions in the ocean. The hypothesized responses to these environmental conditions are consistent with responses of Cenozoic foraminifera to global cooling and sea level fall. The observed morphological change across the PPB is consistent with these hypothesized responses to environmental changes, with the exception of salinity levels, indicating a cooling period across the PPB that has been proposed by other studies.

This change is replicated in all four studied basins in the Central and Southwestern United States across the PPB. The east to west gradient of the intensity of the morphological change could be indicative of basin specific responses to sea level change, nutrient levels and salinity, indicating that the signal could be lost under certain conditions.

This change can be used to identify the PPB in the Central and Southwestern United States, because it is independent of species identification and prior rock age association. However, while this change is restricted to *Triticites*, similar responses to environmental changes could be seen in other fusulinid groups as well as other foraminiferan groups from other periods of time where significant changes in environment occur.

REFERENCES

Arefifard, Sakineh. 2018. “Morphometric analysis of Middle Permian *Eopolydiexodina* and *Monodiexodina* species from the Dalan Formation, Zard-Kuh Mountains, Zagros, Iran: An integration of traditional approach and quantitative analyses to identify fusulinid species.” *Geological Journal* 54, no. 4 (June): 2288-2300. https://doi.org/10.1002/gj.3297

Beavington-Penney, Simon J., and Andrew Racey. 2004. “Ecology of extant nummulitids and other larger benthic foraminifera: applications in palaeoenvironmental analysis.” *Earth-Science Reviews* 67, no. 3-4 (February): 219-265. DOI: 10.1016/j.earscirev.2004.02.005

Boudaugher-Fadel, Marcelle K. 2018. *Evolution and geological significance of larger benthic foraminifera*. London, England: UCL Press. https://doi.org/10.14324/111.9781911576938

Bradshaw, John S. 1957. “Laboratory Studies on the Rate of Growth of the Foraminifer, *Streblus beccarii* (Linné) var. *tepida* (Cushman).” *Journal of Paleontology* 31, no. 6 (November): 1138-1147.

Brett, Carlton E. 1998. “Sequence stratigraphy, paleoecology, and evolution; biotic clues and responses to sea-level fluctuations.” *Palaios* 13, no. 3 (June): 241-262. https://doi.org/10.2307/3515448.

Budd, Ann F. 1990. “Longterm patterns of morphological variation within and among species of reef-corals and their relationship to sexual reproduction.” *Systematic Botany* 15, no. 1 (January-March): 150-165.

Caval-Holme, Franklin, Jonathan Payne, and Jan M. Skotheim. 2013. “Constraints on the adult-offspring size relationship in protists.” *Evolution* 67, no. 12 (June): 3537-3544. DOI: 10.1111/evo.12210

Charnov, Eric L., and SK Morgan Ernest. 2006. “The offspring-size/clutch-size trade-off in mammals.” *The American Naturalist* 167, no. 4 (April): 578-582.

Ciampaglio, Charles N. 2002. “Determining the role that ecological and developmental constraints play in controlling disparity: examples from the crinoid and blastozoan fossil record.” *Evolution & Development* 4, no. 3 (May-June): 170-188. DOI: 10.1046/j.1525-142X.2002.02001.x.

Colorado Plateau Geosystems Inc. *North American Key Time Slices ©2013 Colorado Plateau Geosystems Inc*. 47 maps, JPEG, 4762x5956 pixels, List of references.

Denayer, Julien. 2015. “Rugose corals at the Tournaisian–Viséan transition in the Central Taurides (S Turkey)–Palaeobiogeography and palaeoceanography of the Asian Gondwana margin.” *Journal of Asian Earth Sciences* 98 (November): 371-398. http://dx.doi.org/10.1016/j.jseaes.2014.11.008

DiMichele, William A., Neil J. Tabor, Dan S. Chaney, and W. John Nelson. 2006. “From wetlands to wet spots: Environmental tracking and the fate of Carboniferous elements in Early Permian tropical floras.” *Special Paper of Geological Society of America* 399: 223-248.

Dommergues, Jean-Louis, Sophie Montuire, and Pascal Neige. 2002. “Size patterns through time: the case of the Early Jurassic ammonite radiation.” *Paleobiology* 28, no. 4 (Autumn): 423-434.

Dunbar, Carl O. and G.E. Condra. 1927. “The Fusulinidae of the Pennsylvanian System in Nebraska.” *Bulletin of the Nebraska Geological Survey* 2, series 2: 1-135. Printed by the authority of the State of Nebraska.

Dunbar, Carl O. and John W. Skinner. 1937. “Part 2 Permian Fusulinidae of Texas” In *The Geology of Texas, Volume III Upper Paleozoic Ammonites and Fusulinids*. University of Texas Bulletin 3701: 519-825.

Erwin, Douglas H. 2007. “Disparity: morphological pattern and developmental context.” *Palaeontology* 50, no. 1 (January): 57-73. https://doi.org/10.1111/j.1475-4983.2006.00614.x.

Flake, Ryan Christopher. 2012. “Circulation of North American epicontinental seas during the Carboniferous using stable isotope and trace element analyses of brachiopod shells.” Master’s thesis, Texas A & M University.

Foote, Mike. 1989. “Perimeter-based Fourier analysis: a new morphometric method applied to the trilobite cranidium.” *Journal of Paleontology* 63, no. 6 (November): 880-885.

Foote, Mike. 1999. “Morphological diversity in the evolutionary radiation of Paleozoic and post-Paleozoic crinoids.” *Supplement: Paleobiology Memoirs, Paleobiology* 25, no. 2 (Spring): 1-115.

Gaswirth, Stephanie B. 2017. “Assessment of continuous oil resources in the Wolfcamp shale of the Midland Basin, Permian Basin Province, Texas, 2016.” *US Geological Survey* No. 2017-1013.

Grossman, Ethan L. 2012. “Applying oxygen isotope paleothermometry in deep time.” In *Reconstructing Earth’s Deep-Time Climate—The State of the Art in 2012, Paleontological Society Short Course,* edited by Linda C. Ivany and Brian T. Huber, *The Paleontological Society Papers* 18 (November): 39-67. https://doi.org/10.1017/S1089332600002540

Groves, John R., and Stacey Reisdorph. 2009. “Multivariate morphometry and rates of morphologic evolution within the Pennsylvanian fusulinid *Beedeina* (Ardmore Basin, Oklahoma, USA).” *Palaeoworld* 18, no. 2-3 (December): 120-129. https://dx.doi.org/10.1016/j.palwor.2008.12.001

Groves, John R., and Yue Wang. 2013. “Timing and size selectivity of the Guadalupian (Middle Permian) fusulinoidean extinction.” *Journal of Paleontology* 87, no. 2 (March): 183-196.

Groves, John R., Madison Pike, and Kasey Westley. 2012. “A test for the possibility of photosymbiosis in extinct fusuline Foraminifera: Size and shape related to depth of habitat.” *Palaios* 27, no. 9-10 (September-October): 738-751. DOI: 10.2110/palo.2012.pl.

Harney, Jodi N., Pamela Hallock, and Helen K. Talge. 1998. “Observations on a trimorphic life cycle in *Amphistegina gibbosa* populations from the Florida

Keys." *Journal of Foraminiferal Research* 28, no. 2 (April): 141-147. https://doi.org/10.2113/gsjfr.28.2.141.

Hay, William W., Areg Migdisov, Alexander N. Balukhovsky, Christopher N. Wold, Sascha Flögel, and Emanuel Söding. 2006. "Evaporites and the salinity of the ocean during the Phanerozoic: Implications for climate, ocean circulation and life." *Palaeogeography, Palaeoclimatology, Palaeoecology* 240, no. 1-2 (October): 3-46. https://doi.org/10.1016/j.palaeo.2006.03.044.

Henderson, C.M., V.I. Davydov, and B.R. Wardlaw; contributors: F.M. Gradstein and O. Hammer. 2012. "Chapter 24-The Permian Period." In *The Geologic Time Scale 2012*. Gradstein, Felix M. Edited by James George Ogg, Mark Schmitz, and Gabi Ogg. Elsevier. DOI: 10.1016/B978-0-444-59425-9.00024-X.

Hohenegger, Johann. 2009. "Functional shell geometry of symbiont-bearing benthic foraminifera." *Galaxea, Journal of Coral Reef Studies* 11, no. 2: 81-89.

Hottinger, L. 1982. "Larger foraminifera, giant cells with a historical background." *Naturwissenschaften* 69, no. 8: 361-371.

Jarek, Slawomir. 2012. *mvnormtest: Normality test for multivariate variables*. R package version 0.1-9. https://CRAN.R-project.org/package=mvnormtest.

Keating-Bitonti, Caitlin R., and Jonathan L. Payne. 2018. "Environmental influence on growth history in marine benthic foraminifera." *Paleobiology* 44, no. 4 (September): 736-757. https://doi.org/10.1017/pab.2018.19.

King, Philip Burke, 1930. "The geology of the Glass Mountains, Texas, Pt. 1." *Texas University Bulletin* 3038: 1-167.

King, Philip Burke, 1937. “Geology of the Marathon region, Texas.” *U.S. Geol. Survey Professional Paper* 187:1-148.

Koch, Jesse T., and Tracy D. Frank. 2011. “The Pennsylvanian–Permian transition in the low-latitude carbonate record and the onset of major Gondwanan glaciation.” *Palaeogeography, Palaeoclimatology, Palaeoecology* 308, no. 3-4 (August): 362-372. DOI: 10.1016/j.palaeo.2011.05.041

Koch, Jesse T., and Tracy D. Frank. 2012. “Imprint of the Late Palaeozoic Ice Age on stratigraphic and carbon isotopic patterns in marine carbonates of the Orogrande Basin, New Mexico, USA.” *Sedimentology* 59, no. 1: 291-318. DOI: 10.1111/j.1365-3091.2011.01258.x.

Koepnick, Richard B., and Roger L. Kaesler. 1971. “Intraspecific variation of morphology of *Triticites cullomensis* (Fusulinacea), a statistical analysis.” *Journal of Paleontology* 45, no. 5 (September): 881-887.

Koepnick, Richard B., and Roger L. Kaesler. 1974. “Character correlations and morphologic variations of *Triticites cullomensis* (Fusulinacea).” *Journal of Paleontology* 48, no. 1 (January): 36-40.

Lipps, Jere H. 1982. “Biology/paleobiology of foraminifera.” *Studies in geology, notes for a short course 6* (July): 1-21. https://doi.org/10.1017/S0271164800000476.

Lockwood, Rowan. 2004. “The K/T event and infaunality: morphological and ecological patterns of extinction and recovery in veneroid bivalves.” *Paleobiology* 30, no. 4 (Autumn): 507-521.

Lucas, Spencer G., Karl Krainer, James E. Barrick, Daniel Vachard, and Scott M. Ritter. 2017a. “Lithostratigraphy and microfossil biostratigraphy of the Pennsylvanian lower Permian Horquilla Formation at New Well Peak, Big Hatchet Mountains, New Mexico, USA.” *Stratigraphy* 14, nos. 1-4: 223-246.

Lucas, Spencer G., Karl Krainer, and Daniel Vachard. 2017b. “The Newwellian Substage of the Wolfcampian Stage in the southwestern United States.” *Permophiles* 64 (January): 13-19.

McGowan, Alistair J. 2004. “Ammonoid taxonomic and morphologic recovery patterns after the Permian–Triassic.” *Geology* 32, no. 8 (August): 665-668. https://doi.org/10.1130/G20462.1.

Mitteroecker, Philipp, and Fred Bookstein. 2011. “Linear discrimination, ordination, and the visualization of selection gradients in modern morphometrics.” *Evolutionary Biology* 38, no. 1 (February): 100-114. https://doi.org/10.1007/s11692-011-9109-8.

Montañez, Isabel P., Neil J. Tabor, Deb Niemeier, William A. DiMichele, Tracy D. Frank, Christopher R. Fielding, John L. Isbell, Lauren P. Birgenheier, and Michael C. Rygel. 2007. “CO2-forced climate and vegetation instability during Late Paleozoic deglaciation.” *Science* 315, no. 5808 (January): 87-91. DOI: 10.1126/science.1134207.

Nigam, Rajiv, and Aradhana S. Rao. 1987. “Proloculus size variation in Recent benthic foraminifera: Implications for paleoclimatic studies.” *Estuarine, Coastal and Shelf Science* 24, no. 5: 649-655. https://doi.org/10.1016/0272-7714(87)90104-1.

Olszewski, Thomas D., and Mark E. Patzkowsky. 2003. “From cyclothems to sequences: the record of eustasy and climate on an icehouse epeiric platform (Pennsylvanian-Permian, North American Midcontinent).” *Journal of Sedimentary Research* 73, no. 1 (January): 15-30. https://doi.org/10.1306/061002730015.

Patzkowsky, Mark E., and Steven M. Holland. 2012. *Stratigraphic paleobiology: understanding the distribution of fossil taxa in time and space*. Chicago, Illinois: University of Chicago Press.

Payne, Jonathan L., Adam B. Jost, Steve C. Wang, and Jan M. Skotheim. 2013. “A shift in the long-term mode of foraminiferan size evolution caused by the end-Permian mass extinction.” Evolution: *International Journal of Organic Evolution* 67, no. 3 (August): 816-827. https://doi.org/10.1111/j.1558-5646.2012.01807.x.

R Core Team. 2018. “R: A language and environment for statistical computing.” *R Foundation for Statistical Computing*, Vienna, Austria. URL: https://www.R-project.org/.

Rasband, W.S. 1997-2018. “ImageJ.” *U. S. National Institutes of Health*, Bethesda, Maryland, USA. https://imagej.nih.gov/ij/.

Ross, Charles A. 1959. “The Wolfcamp series (Permian) and new species of fusulinids, Glass Mountains, Texas.” *Journal of the Washington Academy of Sciences* 49, no. 9 (October-November): 299-316.

Ross, Charles Alexander. 1963. “Standard Wolfcampian Series (Permian), Glass Mountains, Texas.” *Geological Society of America* 88: 1-197.

Ross, Charles A. 1965. “Late Pennsylvanian Fusulinidae from the Gaptank Formation, west Texas.” *Journal of Paleontology* 39, no. 6 (November): 1151-1176.

Ross, Charles A. 1972. “Paleobiological analysis of fusulinacean (Foraminiferida) shell morphology.” *Journal of Paleontology* 46, no. 5 (September): 719-728.

Ross, C. A. 1995. “Permian fusulinaceans.” In *The Permian of Northern Pangea*, 167-185. Berlin, Heidelberg: Springer.

Ross, Charles A., and June RP Ross. 1985. “Carboniferous and early Permian biogeography.” *Geology* 13, no. 1 (January): 27-30. https://doi.org/10.1130/0091-7613(1985)13%3C27:CAEPB%3E2.0.CO;2.

Ross, Charles A., and June RP Ross. 1994. “Permian sequence stratigraphy and fossil zonation.” *Canadian Society of Petroleum Geologists Memoir* 17: 219-231.

Ross, Charles A., and June RP Ross. 2003. “Sequence evolution and sequence extinction: fusulinid biostratigraphy and species-level recognition of depositional sequences, Lower Permian, Glass Mountains, West Texas, USA.” *Micropaleontologic Proxies for Sea-level Change and Stratigraphic Discontinuities, Society of Economic Paleontologists and Mineralogists Special Publication* 75: 317-359.

Sabins Jr, Floyd F., and Charles A. Ross. 1963. “Late Pennsylvanian-early Permian fusulinids from southeast Arizona.” *Journal of Paleontology* 37, no. 2 (March): 323-365.

Schmidt, Daniela N., Ellen Thomas, Elisabeth Authier, David Saunders, and Andy Ridgwell. 2018. “Strategies in times of crisis—insights into the benthic

foraminiferal record of the Palaeocene–Eocene Thermal Maximum." *Philosophical Transactions of the Royal Society A: Mathematical, Physical and Engineering Sciences* 376, no. 2130 (July): http://dx.doi.org/10.1098/rsta.2017.0328.

Shi, Yukun, and Norman MacLeod. 2016. "Identification of life-history stages in fusulinid foraminifera." *Marine Micropaleontology* 122 (December): 87-98. http://dx.doi.org/10.1016/j.marmicro.2015.12.002.

Soreghan, Gerilyn S., Andrew M. Moses, Michael J. Soreghan, Michael A. Hamilton, C. Mark Fanning, and Paul K. Link. 2007. "Palaeoclimatic inferences from upper Palaeozoic siltstone of the Earp Formation and equivalents, Arizona-New Mexico (USA)." *Sedimentology* 54, no. 3: 701-719. https://doi.org/10.1111/j.1365-3091.2007.00857.x.

Soreghan, Gerilyn S., Nicholas G. Heavens, Linda A. Hinnov, Sarah M. Aciego, and Carl Simpson. 2015. "Reconstructing the dust cycle in deep time: The case of the late Paleozoic icehouse." In: *Earth-Life Transitions: Paleobiology in the Context of Earth System Evolution*, edited by P. David Polly, Jason J. Head, and David L. Fox, *The Paleontological Society Papers* 21 (October): 83-120. https://doi.org/10.1017/S1089332600002977.

Strauss, Richard E. 2010. "Discriminating groups of organisms." In *Morphometrics for nonmorphometricians*, pp. 73-91. Berlin, Heidelberg: Springer.

Thompson, Marcus Luther. 1948. "Studies of American fusilinids." *The University of Kansas Paleontological Contributions, Protozoa* 1: 1-184.

Thompson, Marcus Luther. 1954. “American Wolfcampian fusulinids.” *The University of Kansas Paleontological Contributions, Protozoa* 5: 1-226.

Torres-Silva, Ana I., Wolfgang Eder, Johann Hohenegger, and Antonino Briguglio. 2018. “Morphometric analysis of Eocene nummulitids in western and central Cuba: taxonomy, biostratigraphy and evolutionary trends.” *Journal of Systematic Palaeontology* 17, no. 7 (April): 557-595. https://doi.org/10.1080/14772019.2018.1446462.

Vachard, Daniel, Lucie Pille, and Jérémie Gaillot. 2010. “Palaeozoic Foraminifera: systematics, palaeoecology and responses to global changes.” *Revue de micropaléontologie* 53, no. 4 (October-December): 209-254. https://doi.org/10.1016/j.revmic.2010.10.001.

Venables, W.N. and B.D. Ripley. 2002. *Modern Applied Statistics with S*. Fourth Edition. New York: Springer. ISBN 0-387-95457-0.

Wahlman, Gregory P. 2013. “Pennsylvanian to Lower Permian (Desmoinesian–Wolfcampian) fusulinid biostratigraphy of Midcontinent North America.” *Stratigraphy* 10, no. 1-2: 73-104.

Wilde, G. L. 2002. “The Newwellian substage: rejection of the Bursumian Stage.” *Permophiles* 41: 53-62.

Wilde, Garner L. 2006. “Pennsylvanian-Permian Fusilinaceans of the Big Hatchet Mountains, New Mexico.” *New Mexico Museum of Natural History and Science Bulletin* 38: 1-331.

Wilkinson, M., 1995. “A comparison of two methods of character construction.” *Cladistics* 11: 297-308.

Williams, Thomas Ellis. 1963. *Fusulinidae of the Hueco Group (Lower Permian) Hueco Mountains, Texas*. New Haven, Connecticut: Peabody Museum, Yale University.

Zhang, Yi-Chun, and Yue Wang. 2018. “Permian fusuline biostratigraphy.” In *The Permian Timescale*, edited by S.G. Lucas and S.Z. Shen. *Geological Society, London, Special Publications* 450, no. 1: 253-288. https://doi.org/10.1144/SP450.14.

Ziegler, Peter A. 2012. *Evolution of Laurussia: A study in Late Palaeozoic plate tectonics*. Dordrecht, the Netherlands: Kluwer Academic Publishers.

APPENDIX A

CASE STUDY OF THE GRAY LIMESTONE MEMBER IN THE WOLFCAMP HILLS

The initial motivation for this project was to determine the biostratigraphic location of the Pennsylvanian-Permian boundary (PPB) in the Wolfcamp Hills of West Texas. This investigation in the Wolfcamp Hills is actually at the center of a disagreement concerning the stratigraphic ranges of *Triticites* species between Ross (1963) and Wilde (2006). The lithostratigraphic unit under scrutiny, PB King's Bed 2 (King, 1930), also known the Gray Limestone Member (GLM), is where this transition from Pennsylvanian to Permian strata is supposed to occur. Some workers consider the GLM to be earliest Permian (Wilde, 2002), while others consider it to be the uppermost Virgilian (Ross, 1963). Due to the presence of a large unconformity that supposedly spans the PPB in the Wolfcamp Hills, it is unclear whether the informal Newwellian substage proposed by Wilde (2002) is present in the GLM. Within our data set, there were 8 specimens from within the GLM, 13 specimens from below and 19 specimens from above. Using LDA scores for the specimens collected by Ross (1959, 1963, 1965) within the GLM as well as above and below, we can determine if the GLM is closer in morphological signal to those strata above or below it.

The median LDA score of specimens from PB King's Bed 2 or the Gray Limestone Member (GLM) was more similar to the scores of specimens above the GLM than below (**Appendix Figure 1**). While these results do not resolve the debate as to

whether the Newwellian substage is present in the Wolfcamp Hills and/or if it is the lowest part of the Wolfcampian substage, we can say that the morphologies of specimens within the GLM as a whole are more similar to strata in the Nealian substage. More data from the GLM needs to be analyzed and compared with the position of each specimen within the GLM to determine if the position of this transition is at the base of or within the GLM.

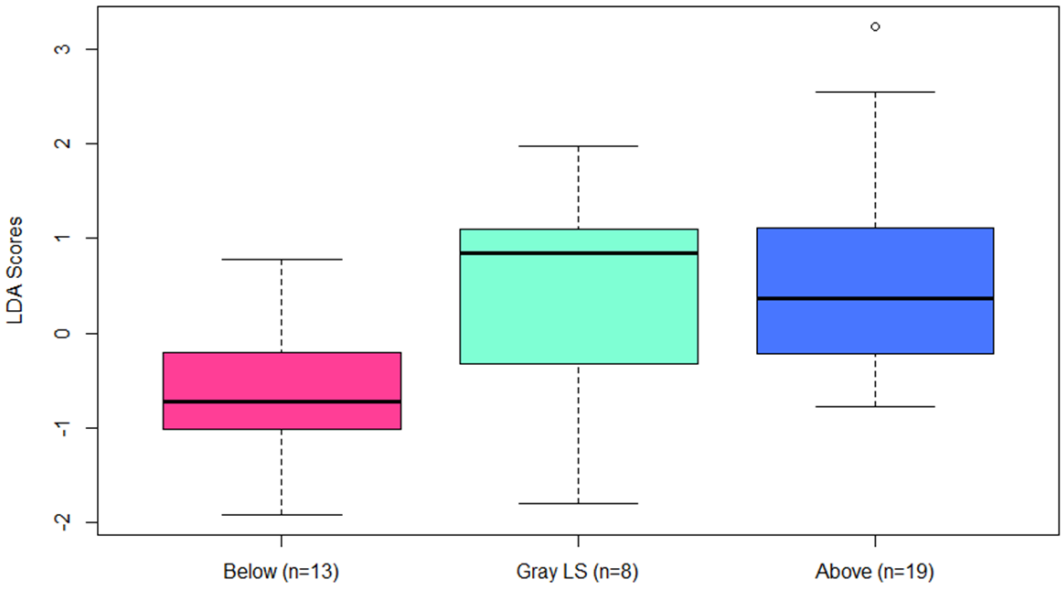

Appendix Figure 1: LDA scores of Triticites specimens from below, above, and within the Gray Limestone Member (Gray LS) published in Ross, 1959, 1963, 1965. Shaded box represents the interquartile range (IQR). Lower box bound represents the 25th percentile (Q1) and the upper box bound represents the 75th percentile (Q3). Lower whisker represents the minimum values outside the IQR (Q1-1.5*IQR). Upper whisker represents the maximum values outside the IQR (Q3+1.5*IQR). Circles outside whiskers are the outliers. Thick middle line represents the median LDA score.

APPENDIX B

MORPHOLOGICAL DISTINCTIVENESS

B.1. Methods

If species are quantitatively distinct, they are more useful to biostratigraphy. However, a common result of evolution is the increase in distinctness over time (Brett, 2015). Since *Triticites* is thought to be the ancestor of later Permian fusulinids, it is important to determine if *Triticites* species are becoming more morphologically distinct. Discreteness index (DI) is used to determine how tightly clustered conspecific specimens are and how spread out those clusters are (i.e. how distinct species are relative to each other) (Foote, 1989). Discreteness index (DI) is defined by the following equation, DI = AD/WD, where AD is the among-group dispersion and WD is the within-group dispersion. Among-group dispersion (AD) is defined as "the mean of all pairwise distances between group centroids" (Foote, 1989) and within-group dispersion (WD) is defined as "the mean of all pairwise distances between samples within a group (higher taxon)" (Foote, 1989). AD, WD and DI were all calculated for the Virgilian and Newwellian-Nealian using the size-standardized, transformed data. Since some species are found in both time bins, only the specimens found in a particular time bin are used for the calculation of that time bin. Similarly, since other species are only found in one of the two time bins, those species are only included in the calculation of the time bin within which they were found. *Triticites meeki* was excluded from the WD calculation for the Virgilian because there was only one specimen. If DI > 1, then within-group

dispersion is smaller than among-group dispersion (WD < AD), indicating more morphological variation between groups than within groups. If DI < 1, then within-group dispersion is larger than among-group dispersion (WD > AD), indicating more morphological variation within groups than between groups. Similarly, if Newwellian-Nealian species have a higher DI than Virgilian species, then Newwellian-Nealian species have more distinct morphologies than Virgilian species.

B.2. Results

Calculations of AD and WD for the Virgilian and Newwellian-Nealian reveal that Newwellian-Nealian conspecifics have a smaller WD and a larger AD than Virgilian conspecifics (**Appendix Table 1**). Further, the DI for Newwellian-Nealian conspecifics is higher than the DI for Virgilian conspecifics (**Appendix Table 1**). However, since within-group dispersion is larger than among-group dispersion (WD > AD) in both the Virgilian and Newwellian-Nealian, there is still more morphological variation within species than between species.

Appendix Table 1: Within-group dispersion (WD), among-group dispersion (AD), and discreteness index (DI) for each time bin using the size-standardized untransformed data.

Time Bin	WD	AD	DI
Virgilian	4.751978	2.770195	0.582956
Newwellian-Nealian	3.855419	2.984834	0.774192

B.3. Discussion

Morphological distinctness or disparity has long been associated as the filling of "empty niches" after times of crisis or mass extinctions (Foote, 1999; Ciampaglio, 2002; Dommergues et al., 2002; Lockwood, 2004; McGowan, 2004, Erwin, 2007). This observation with other taxa is similar to the morphological response to habitat loss due to global cooling and sea level fall (Ross, 1972; Groves and Wang, 2013). During this time of crisis, the Virgilian-type fusulinids would have to adapt to fill in open niches created by the drop in sea level. To do this, fusulinids would develop new morphologies to help them survive in the new niche. This would allow them to "branch out" in their morphologies and claim a specific morphospace, giving rise to the Newwellian-Nealian-type fusulinids. This "branch out" would result in a smaller WD and a larger AD, which is consistent with the WD and AD values from the Newwellian-Nealian specimens.

In addition, studies of morphological variation within species of reef corals showed that species with less within-species variation (therefore, higher disparity) were mostly asexual reproducers (Budd, 1990). This is consistent with the observed morphologies of Newwellian-Nealian specimens that show evidence of asexual reproduction also show less within-species variation (**Table 5**).